CHARACTERISTICS OF THE EQUATORIAL IONOSPHERIC E-LAYER IN ILORIN

Ojerheghan, G.I.[1*]
[1]*Department of Physics, Faculty of Physical Sciences, University of Ilorin, Nigeria*
**godfrey777@gmail.com*

ABSTRACT

The E-layer is one of the layers in the ionosphere which aids medium wave radio propagation. The auto-scaled parameters used were obtained from the Digisonde Portable Sounder DPS4 at the University of Ilorin, an equatorial station. The parameters (data) used are f_oE, f_oEs, h_mE, h`E and h`Es. Diurnal and seasonal effects on these parameters were studied for the year 2010.

The results obtained showed that the regular E-layer becomes noticeable at sunrise (about 0600UT) and attains its peak value at noon time between 1100UT and 1200UT and later becomes undetectable by the sounder at sunset; between 1700UT and 1800UT. There were seasonal effects observed in the pattern of the regular E-layer. The f_oEs and h`Es of sporadic E was higher than the $f_oE$, $h_mE$ and h`E of the regular or normal E respectively. The approximate true height range of the E layer was well established between 100.45km to 113.43km and it was seen that the maximum electron density occurred at 101.94km and the maximum frequency f_oE was 3.54MHz. These frequencies and heights can be used as guide for the establishment of TV or radio stations.

Keywords: equinox, solstice, sporadic E, seasonal variation, critical frequency, ionograms, earth's atmosphere

CHAPTER ONE

INTRODUCTION

1.0 THE CONCEPT AND NATURE OF THE EARTH'S ATMOSPHERE

The atmosphere surrounds Earth and protects us by blocking out dangerous rays from the sun. The atmosphere is a mixture of gases that becomes thinner until it gradually reaches space. It is composed of Nitrogen (78%), Oxygen (21%), and other gases (1%).

Oxygen is essential to life because it allows us to breathe. Some of the oxygen has changed over time to ozone. The ozone layer filters out the sun's harmful rays. Recently, there have been many studies on how humans have caused a hole in the ozone layer.

Humans are also affecting Earth's atmosphere through the greenhouse effect. Due to increases in gases, like carbon dioxide, that trap heat being radiated from the Earth, scientists believe that the atmosphere is having trouble staying in balance creating the greenhouse effect (Randy R., 2003)

The atmosphere is divided into five layers depending on how temperature changes with height. Most of the weather occurs in the first layer.

1.1 LAYERS OF THE EARTH'S ATMOSPHERE

The atmosphere is divided into five layers. It is thickest near the surface and thins out with height until it eventually merges with space. The troposphere is the first layer above the surface and contains half of the Earth's atmosphere. Weather occurs in this layer. Many jet aircrafts fly in the stratosphere because it is very stable. Also, the ozone layer absorbs harmful rays from the Sun. Meteors or rock fragments burn up in the mesosphere. The thermosphere is a layer with auroras. It is also where the space shuttle orbits. The atmosphere merges into space in the extremely thin exosphere. This is the upper limit of our atmosphere.

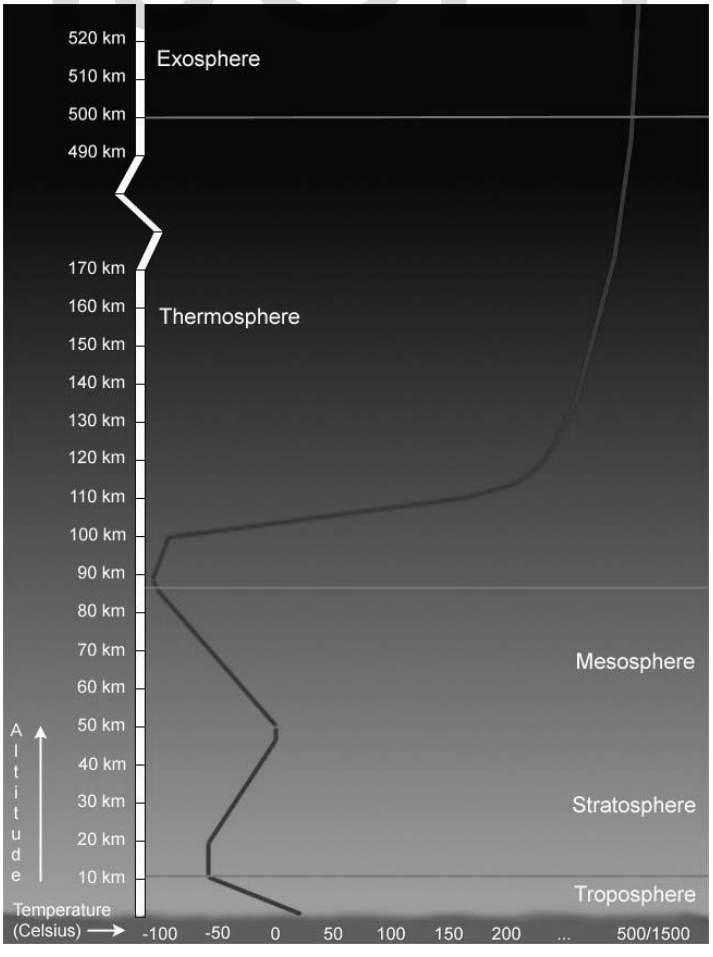

Fig1.1: The Average Temperature Profile of Earth's Atmosphere (http://windows2universe.org)

1.1.1 The Troposphere

The troposphere is the lowest layer of the Earth's atmosphere. The air is very well mixed and the temperature decreases with altitude.

Air in the troposphere is heated from the ground up. The surface of the Earth absorbs energy and heats up faster than the air does. The heat is spread through the troposphere because the air is slightly unstable. Weather occurs in the Earth's troposphere.

1.1.2 The Stratosphere

In the Earth's stratosphere, the temperature increases with altitude. On Earth, ozone causes the increasing temperature in the stratosphere. Ozone is concentrated around an altitude of 25 kilometers. The ozone molecules absorb dangerous kinds of sunlight, which heats the air around them. The stratosphere is located above the top of the troposphere.

1.1.3 The Mesosphere

In the Earth's mesosphere, the air is relatively mixed together and the temperature decreases with altitude. The atmosphere reaches its coldest temperature of around -90°C in the mesosphere. This is also the layer in which a lot of meteors burn up while entering the Earth's atmosphere. The mesosphere is on top of the stratosphere. The upper parts of the atmosphere, such as the mesosphere, can sometimes be seen by looking at the very edge of a planet.

1.1.4 The Thermosphere

The thermosphere is the fourth layer of the Earth's atmosphere and is located above the mesosphere. The air is really thin in the thermosphere. A small change in energy can cause a large

change in temperature. That's why the temperature is very sensitive to solar activity. When the sun is active, the thermosphere can heat up to 1,500°C or higher.

The Earth's thermosphere also includes the region of the atmosphere called the ionosphere. The ionosphere is a region of the atmosphere that is filled with charged particles. The high temperatures in the thermosphere can cause molecules to ionize. This is why an ionosphere and thermosphere can overlap.

1.1.5 The Exosphere

Very high up, the Earth's atmosphere becomes very thin. The region where atoms and molecules escape into space is referred to as the exosphere. The exosphere is on top of the thermosphere.

1.1.6 The Ionosphere

Scientists call the ionosphere an extension of the thermosphere. So technically, the ionosphere is not another atmospheric layer. The ionosphere represents less than 0.1% of the total mass of the Earth's atmosphere. Even though it is such a small part, it is extremely important.

The upper atmosphere is ionized by solar radiation. That means the Sun's energy is so strong at this level, that it breaks apart molecules. So there ends up being electrons floating around and molecules which have lost or gained electrons. When the Sun is active, more and more ionization happens.

Different regions of the ionosphere make long distance radio communication possible by reflecting the radio waves back to Earth. It is also home to auroras. Temperatures in the ionosphere just keep getting hotter as you go up.

1.2 REGIONS OF THE IONOSPHERE

The ionosphere is broken down into the D, E and F regions. The breakdown is based on what wavelength of solar radiation is absorbed in that region most frequently.

The D region is the lowest in altitude, though it absorbs the most energetic radiation, hard x-rays. The D region doesn't have a definite starting and stopping point, but includes the ionization that occurs below about 90km. The E region peaks at about 105km. It absorbs soft x-rays.

The F region starts around 105km and has a maximum around 600km. It is the highest of all of the regions. Extreme ultra-violet radiation (EUV) is absorbed there.

On a more practical note, the D and E regions reflect AM radio waves back to Earth. Radio waves with shorter lengths are reflected by the F region. Visible light, television and FM wavelengths are all too short to be reflected by the ionosphere. Thus, television stations are made possible by satellite transmissions.

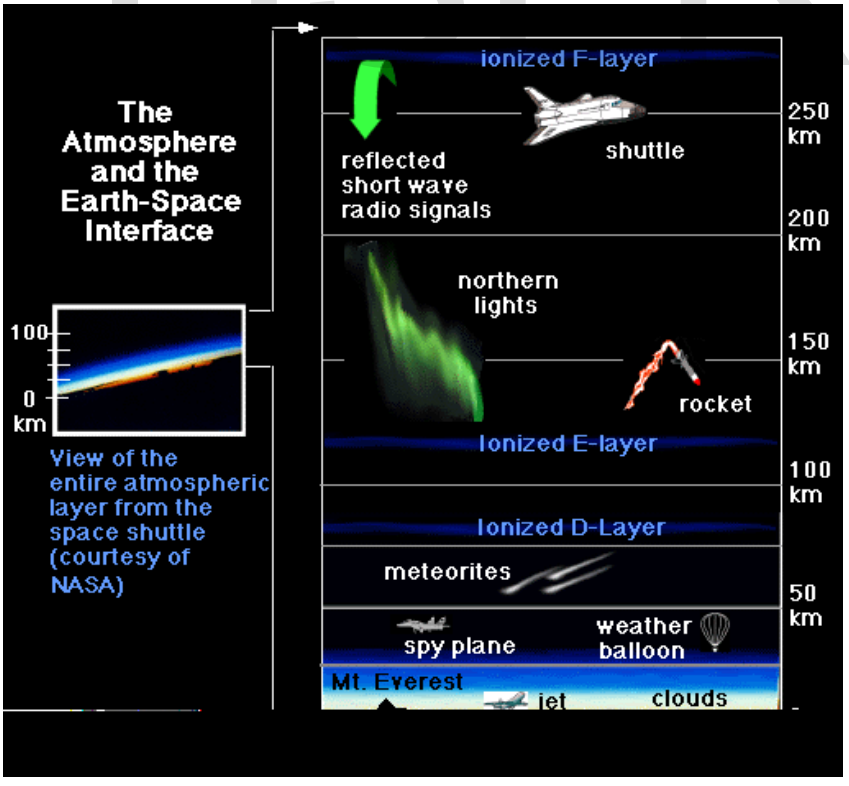

Fig. 1.2: The three typical regions (D, E, and F) in the ionosphere (http://windows2universe.org)

1.3 THE SUN'S EFFECT ON THE IONOSPHERE

Invisible layers of ions and electrons are found in the Earth's atmosphere. We call this region of atmosphere the ionosphere. The main source of these layers is the Sun's ultraviolet light which ionizes atoms and molecules in the Earth's upper atmosphere. During this process, electrons are knocked free from molecules or particles in the atmosphere.

Flares and other big events on the Sun produce increased ultraviolet, x-ray and gamma-ray photons that arrive at the Earth just 8 minutes later (other particles from the Sun may arrive days later) and dramatically increase the ionization that happens in the atmosphere. So, the more active the Sun, the thicker the ionosphere.

It is this solar radiation that ionizes the upper atmosphere, creating the ionosphere. The figure below (Fig. 1.3) shows the different types of radiation in the earth’s atmosphere.

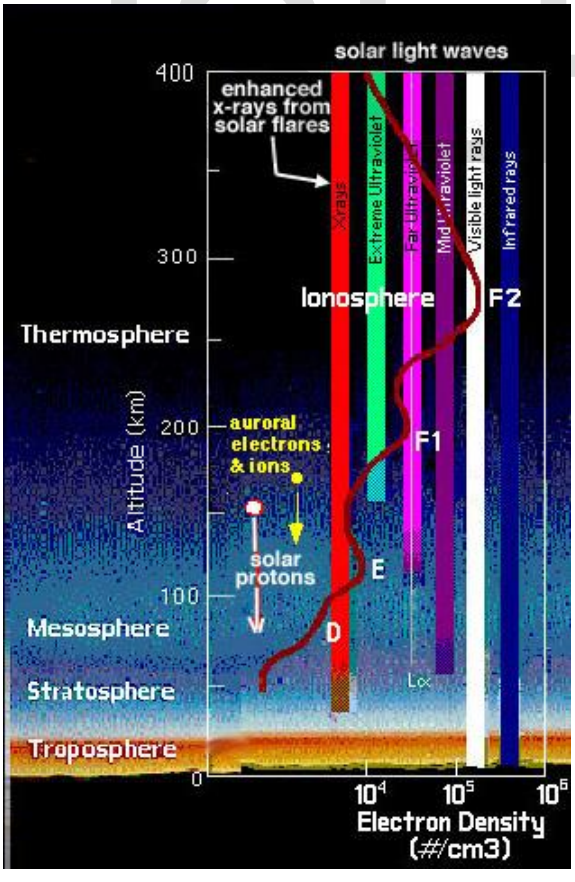

Fig. 1.3: The different types of solar radiation (x-rays to infrared radiation) in the Earth's atmosphere (http://windows2universe.org)

1.4 AIMS AND OBJECTIVES OF PROJECT

The aim of this project is to study the characteristics of the equatorial *E* layer: f_oE, f_oEs, h_mE, $h`E$, $h`E$s and verify its variations and frequency of occurrence at Ilorin in the year 2010.

CHAPTER TWO

LITERATURE REVIEW

2.0 A BRIEF HISTORY OF THE IONOSPHERE

On December 12, 1901, Marconi (a.k.a. “Father of Wireless”) received a signal in St. John’s Newfoundland that had been sent from Cornwall, England (500 kHz) who won a Nobel Prize in physics in 1909 for using EM radiation for radio communication. In 1902, Heaviside and Kennely proposed that a conducting layer existed in upper atmosphere that reflects electromagnetic signals. About that time, a theory was proven that electromagnetic radiation travels in straight lines and maximum distance determined by Line-of-Sight (LOS). With this knowledge, one still doubt how could Marconi have “heard” the signal. In 1924, Appleton developed the ionosonde (ground-based sounding) and proved existence of ionosphere. He was awarded Nobel Prize in physics in 1947

2.1 THE NATURE AND CONCEPT OF IONOSPHERIC E-LAYER

The ionosphere is a part of the upper atmosphere, comprising portions of the mesosphere, thermosphere and exosphere, distinguished because it is ionized by solar radiation. It plays an important part in atmospheric electricity and forms the inner edge of the magnetosphere. It has practical importance because, among other functions, it influences radio propagation to distant places on the Earth (Rawer K., 1993).

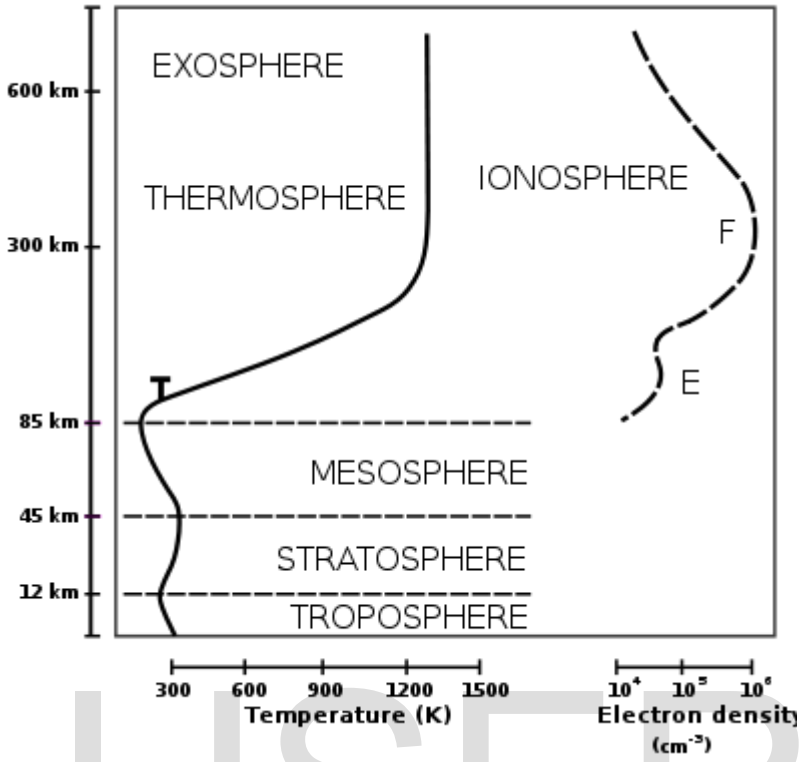

Fig. 2.1: Relationship of the atmosphere and ionosphere (Ionosphere - Wikipedia, the free encyclopedia.htm)

The ionosphere is a shell of electrons and electrically charged atoms and molecules that surrounds the Earth, stretching from a height of about 50 km to more than 1,000 km. It owes its existence primarily to ultraviolet radiation from the sun.

The lowest part of the Earth's atmosphere, the troposphere extends from the surface to about 10 km (6 miles). Above 10 km is the stratosphere, followed by the mesosphere. In the stratosphere incoming solar radiation creates the ozone layer. At heights of above 80 km (50 miles), in the thermosphere, the atmosphere is so thin that free electrons can exist for short periods of time before they are captured by a nearby positive ion.

The number of these free electrons is sufficient to affect radio propagation. This portion of the atmosphere is ionized and contains a plasma which is referred to as the ionosphere. In a plasma, the

negative free electrons and the positive ions are attracted to each other by the electromagnetic force, but they are too energetic to stay fixed together in an electrically neutral molecule.

Ultraviolet (UV), X-Ray and shorter wavelengths of solar radiation are ionizing, since photons at these frequencies contain sufficient energy to dislodge an electron from a neutral gas atom or molecule upon absorption. In this process the light electron obtains a high velocity so that the temperature of the created electronic gas is much higher (of the order of thousand K) than the one of ions and neutrals. The reverse process to Ionization is recombination, in which a free electron is "captured" by a positive ion, occurs spontaneously. This causes the emission of a photon carrying away the energy produced upon recombination. As gas density increases at lower altitudes, the recombination process prevails, since the gas molecules and ions are closer together. The balance between these two processes determines the quantity of ionization present.

Ionization depends primarily on the Sun and its activity. The amount of ionization in the ionosphere varies greatly with the amount of radiation received from the sun. Thus there is a diurnal (time of day) effect and a seasonal effect. The local winter hemisphere is tipped away from the Sun, thus there is less received solar radiation. The activity of the sun is associated with the sunspot cycle, with more radiation occurring with more sunspots (Yuen, 1966).

Radiation received also varies with geographical location (polar, auroral zones, mid-latitudes, and equatorial regions). There are also mechanisms that disturb the ionosphere and decrease the ionization. There are disturbances such as solar flares and the associated release of charged particles into the solar wind which reaches the Earth and interacts with its geomagnetic field (Yenne, 1985).

2.2 THE IONOSPHERIC LAYERS

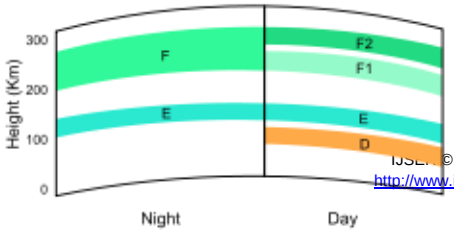

Fig. 2.2: Ionospheric layers (Ionosphere - Wikipedia, the free encyclopedia.htm)

At night the F layer is the only layer of significant ionization present, while the ionization in the E and D layers is extremely low. During the day, the D and E layers become much more heavily ionized, as does the F layer, which develops an additional, weaker region of ionisation known as the F1 layer. The F2 layer persists by day and night and is the region mainly responsible for the refraction of radio waves.

2.2.1 D LAYER

The D layer is the innermost layer, 60 km to 90 km above the surface of the Earth. Ionization here is due to Lyman series-alpha hydrogen radiation at a wavelength of 121.5 nanometre (nm) ionizing nitric oxide (NO). In addition, with high Solar activity hard X-rays (wavelength < 1 nm) may ionize (N_2, O_2). During the night cosmic rays produce a residual amount of ionization. Recombination is high in the D layer, the net ionization effect is low, but loss of wave energy is great due to frequent collisions of the electrons (about ten collisions every milli-sec). As a result high-frequency (HF) radio waves are not reflected by the D layer but suffer loss of energy therein.

This is the main reason for absorption of HF radio waves, particularly at 10 MHz and below, with progressively smaller absorption as the frequency gets higher. The absorption is small at night and greatest about midday. The layer reduces greatly after sunset; a small part remains due to galactic cosmic rays. A common example of the D layer in action is the disappearance of distant AM broadcast band stations in the daytime.

During solar proton events, ionization can reach unusually high levels in the D-region over high and polar latitudes. Such very rare events are known as Polar Cap Absorption (or PCA) events, because the increased ionization significantly enhances the absorption of radio signals passing through the region. In

fact, absorption levels can increase by many tens of dB during intense events, which is enough to absorb most (if not all) transpolar HF radio signal transmissions. Such events typically last less than 24 to 48 hours.

2.2.2 E LAYER

The E layer is the middle layer, 90 km to 120 km above the surface of the Earth. Ionization is due to soft X-ray (1-10 nm) and far ultraviolet (UV) solar radiation ionization of molecular oxygen (O_2). Normally, at oblique incidence, this layer can only reflect radio waves having frequencies lower than about 10 MHz and may contribute a bit to absorption on frequencies above. However during intense Sporadic E events the Es layer can reflect frequencies up to 50 MHz and higher. The vertical structure of the E layer is primarily determined by the competing effects of ionization and recombination. At night the E layer rapidly disappears because the primary source of ionization is no longer present. After sunset an increase in the height of the E layer maximum increases the range to which radio waves can travel by reflection from the layer.

This region is also known as the Kennelly-Heaviside Layer or simply the Heaviside layer. Its existence was predicted in 1902 independently and almost simultaneously by the American electrical engineer Arthur Edwin Kennelly (1861-1939) and the British physicist Oliver Heaviside (1850-1925). However, it was not until 1924 that its existence was detected by Edward V. Appleton.

2.2.3 Es LAYER

The Es layer (sporadic E-layer) is characterized by small, thin clouds of intense ionization, which can support reflection of radio waves; rarely up to 225MHz. Sporadic-E events may last for just a few minutes to several hours. Sporadic E propagation makes radio amateurs very exited, as propagation paths that are generally unreachable can open up. There are multiple causes of sporadic-E that are still being pursued by researchers.

This propagation occurs most frequently during the summer months when high signal levels may be reached. The skip distances are generally around 1,000km (620miles). Distances for one hop propagation

can be as close as 900km [500miles] or up to 2500km (1,400miles). Double-hop reception over 3,500 km (2,000 miles) is possible (Leo, 1994)

2.2.4 F LAYER

The F layer or region, also known as the Appleton layer extends from about 200km to more than 500km above the surface of Earth. It is the densest point of the ionosphere, which implies signals penetrating this layer will escape into space. Beyond this layer is the topside ionosphere. Here extreme ultraviolet (UV, 10–100nm) solar radiation ionizes atomic oxygen. The F layer consists of one layer at night, but during the day, a deformation often forms in the profile that is labelled F1.

The F2 layer remains by day and night responsible for most sky wave propagation of radio waves, facilitating high frequency (HF or shortwave) radio communications over long distances.

2.3 TYPES OF *E* -LAYER

There are three types of *E*-layer according to their appearances in the ionosonde. They are:

(a) Sporadic *E*: At certain times, however, intense patches of ionisation form in the *E* layer which lasts for a short period of time, a phenomenon known as Sporadic *E*. Incident VHF signals that strike these patches are reflected back to earth thereby cutting off the F1-layer, thus distorting communication signals.

(b) Blanketing *E*: This occurs when there is an ion convergence source. It indicates that the layer is under tensed ionization and there is no significant transmission or meaningful measured parameter.

(c) Regular *E*: This occurs when there is a significant transmission of signals in which there is a clear existence of a higher layer (F-layer).

2.4 CLASSES OF *E* -LAYER

According to the latitudinal variations, the *E*-layer can be described in three major classes as follows:

- Upper latitudinal *E*-layer: This is the layer of *E*-region that exists in upper latitudes both in the North and South which about 90°N to 60°N and 90°S to 60°S.
- Mid-latitudinal *E*-layer: This is the layer of *E*-region that exists in middle latitudes both in the North and South which about 60°N to 20°N and 60°S to 20°S.
- Equatorial *E*-layer: This is the layer of *E*-region that exists in lower latitudes few degrees from the equator both in the North and the South which about 20°N to 0°N and 20°S to 0°S or 20°N to 20°S.

2.5 THE IONOSONDE

An ionosonde or ionospheric sounder (colloq. chirpsounder), is a specialized radar system for the examination of the ionosphere. An ionosonde is used for finding the optimum operation frequencies for broadcasts or two-way communications in the high frequency range.

The term ionosonde was also used in the past to describe a balloon-borne upper atmospheric research device, used in determining the amount of ionizing radiation in the atmosphere caused primarily by nuclear testing (Odishaw, 1961).

2.5.1 AN IRX-58-23 IONOSONDE SYSTEM

Ionospheric reflection of radio waves was discovered in 1924 by Edward Victor Appleton. The basic ionosonde technology was invented in 1925 by Gregory Breit and Merle A. Tuve and further developed in the late 1920s by a number of prominent physicists, including E. V. Appleton. The term ionosphere and, hence, the etymology of its derivatives, was proposed by Robert Watson-Watt. (Appleton, E.V., 1931; Breit, G. and Tuve, M. A., 1926)

An ionosonde consists of:

(i) A high frequency (HF) transmitter, automatically tuneable over a wide range. Typically the frequency coverage is 0.5–23MHz or 1–40MHz, though normally sweeps are confined to approximately 1.6–12MHz.

(ii) A tracking HF receiver which can automatically track the frequency of the transmitter.

(ii) An antenna with a suitable radiation pattern, which transmits well vertically upwards and is efficient over the whole frequency range used.

(iii) A data storage facility used to store recorded ionograms with their parameters.

2.5.2 DIGITAL CONTROL AND DATA ANALYSIS CIRCUITS

The transmitter sweeps all or part of the HF frequency range, transmitting short pulses. These pulses are reflected at various layers of the ionosphere, at heights of 100–400km, and their echos are received by the receiver and analyzed by the control system. The result is displayed in the form of an ionogram (Gwyn, W., 2009).

Modern ionosondes, like the popular Lowell DIGISONDE(TM), use low power transmitters but compensate by using specialized DSP techniques in the receiver. The result is a portable instrument, which can be easily relocated to interesting HF communications sites.

The HAARP Digisonde, which was developed and provided by the University of Massachusetts at Lowell, was one of the first instruments installed at the HAARP Research Station. The purposes of this instrument are to support frequency management of the 3600 kilowatt Ionospheric Research Instrument transmitter and to provide real time ionospheric characteristics for guiding experiment selection. The Digisonde data are processed, archived, and are available for post-analysis of experiment results. Various formats of the information derived from the Digisonde are made available on the HAARP web site in chart form in near real time and can be accessed from the Data Index.

2.5.3 MODE OF OPERATION

As the transmitted frequency increases, the radio wave is refracted less by the ionisation in the layer, and so it penetrates further before it is eventually reflected. As the wave approaches the reflection height, its group velocity approaches zero and this increases the time-of-flight of the signal. Eventually, a frequency is reached that enables the wave to penetrate the layer without being reflected. For ordinary mode waves, this occurs when the transmitted frequency (f_o) just exceeds the peak plasma frequency of the layer. These frequencies are identified by the layer where reflection takes place (f_oE, f_oF1, f_oF2 and f_oEs). In the case of the extraordinary wave, the magnetic field of the earth enhances the reflection capability of the ionosphere and reflection occurs at a frequency (f_x) that is higher than the ordinary wave by half the electron gyro frequency.

The frequency f_c at which a wave just penetrates a layer of ionisation is known as the critical frequency of that layer. The critical frequency is related to the electron density in the specific layer (D, E, F1 or F2).

All transmitted frequencies above this critical frequency will penetrate the layer without being reflected. Their group velocity, however, will be slowed by any ionisation, and this will add to the time-of-flight. If such a wave encounters another layer whose plasma frequency is higher than the frequency of the wave, it will be reflected, and the return signal will be further delayed as it travels back through the underlying ionisation. Therefore, HF frequencies between 5 and 30MHz pass through the E layer and are reflected at the F layer. Similarly, MF frequencies (AM broadcast stations) at night pass through the D layer and are reflected by the E layer. When a sporadic E cloud passes over the ionosonde, then f_oEs becomes very high, often exceeding 25MHz. This high reflection frequency allows medium distance ionospheric communications and TV DX reception in the low VHF range (28, 50 and even 70MHz) with very strong signal strengths (Judd, 1987).

2.6 IONOGRAM

An ionogram is a display of the data produced by the ionosonde. It is a graph of the virtual height of the ionosphere plotted against frequency. Ionograms are often converted into electron density profiles. Data from ionograms may be used to measure changes in the Earth's ionosphere due to space weather events.

The maximum usable frequency (MUF) for radio waves transmitted at a low angle over the horizon is approximate 3 times the highest frequency returned to the ionosonde from radio waves transmitted directly upwards (to the zenith of the location). Therefore, in the sample ionogram shown above, fxI was measured as 8.80 MHz (green dataset), and the MUF for ionospheric reflection at the area of the ionosonde was calculated as 22.6MHz for a hop distance of 3000 km. The pink dataset, which represents the ordinary wave, shows reflections at approximately 3.51MHz (E-layer) and 4.85MHz (F-layer).

This ionogram shows a well-formed F-Layer with a peak ionization at around 180 km. There is also a less obvious E-Layer at an altitude of about 104 km. The ionogram clearly shows how the transmitted digisonde signal splits into reflected ordinary and extraordinary waves. The ionogram chart and the parameter f_oF2 in the list on the left side of the chart, show that the highest frequency that will be reflected from the ionosphere for vertical incidence (i.e., for a radio wave travelling straight up from the ground) is 8.375MHz.

The ionogram also shows what appear to be faint reflections from an altitude of 700 km. In reality, these chart points are the result of the sounder's radar signal being reflected by the ionosphere, returning to the ground where they are reflected back to the ionosphere for a second reflection before being detected by the Digisonde receiver. The time-of-flight is, therefore twice that of the normal reflection and the computed virtual height is twice the normal virtual height. This type of presentation is often seen under conditions of low ionospheric absorption. The figure below is an example of a typical ionogram.

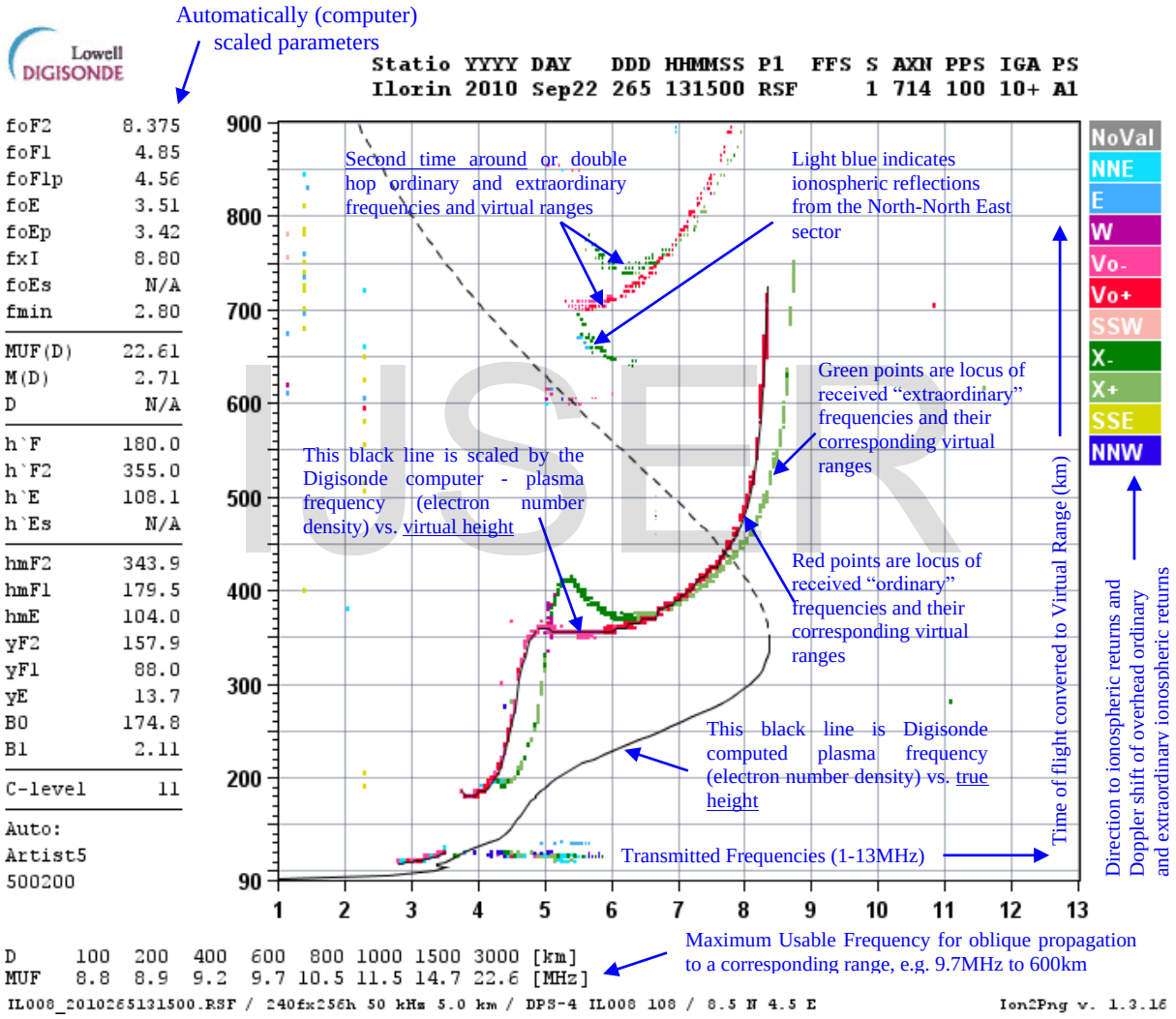

Fig 2.3: An example of typical ionogram (Observatory, University of Ilorin on September 22, 2010 at Lat. 0.5°N, Long. 4.5°E)

2.6.1 IONOGRAM OF BLANKETING *E*

The ionogram of a blanketing *E* indicates the presence of heavy ionisation in E-layer such a way that the F-layer is completely out of traces. In this case, no parameter is measured, showing no significant transmission, hence no value for f_oE nor f_oEs.

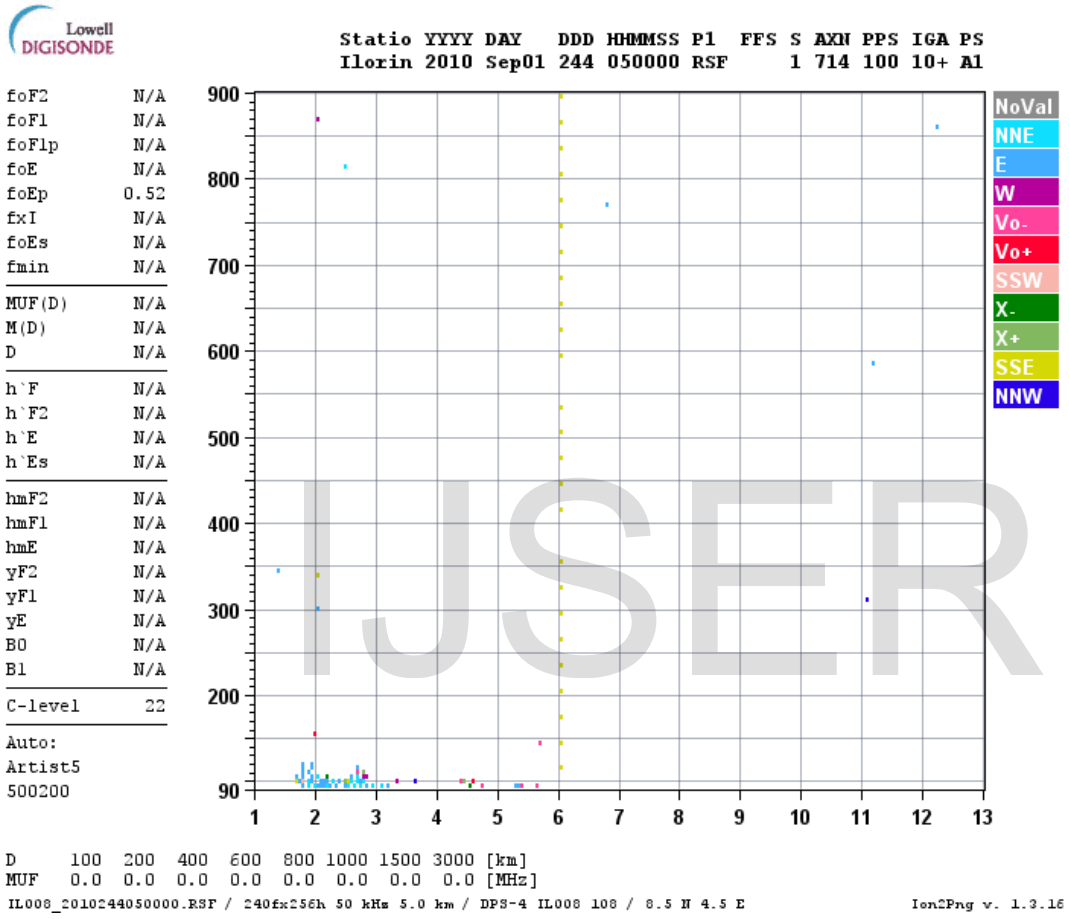

Fig 2.4: An example of typical blanketing E ionogram (Observatory, University of Ilorin on September 1, 2010 at Lat. 0.5°N, Long. 4.5°E).

2.6.2 IONOGRAM OF SPORADIC *E*

The ionogram of a sporadic *E* indicates the presence of unusual intense patches of ionisation form in the E-layer which lasts for a short period of time. Incident VHF signals that strike these patches are reflected back to earth thereby cutting off the F1-layer, thus distorting communication signals. In this case, the value for f_oEs = 3.15MHz.

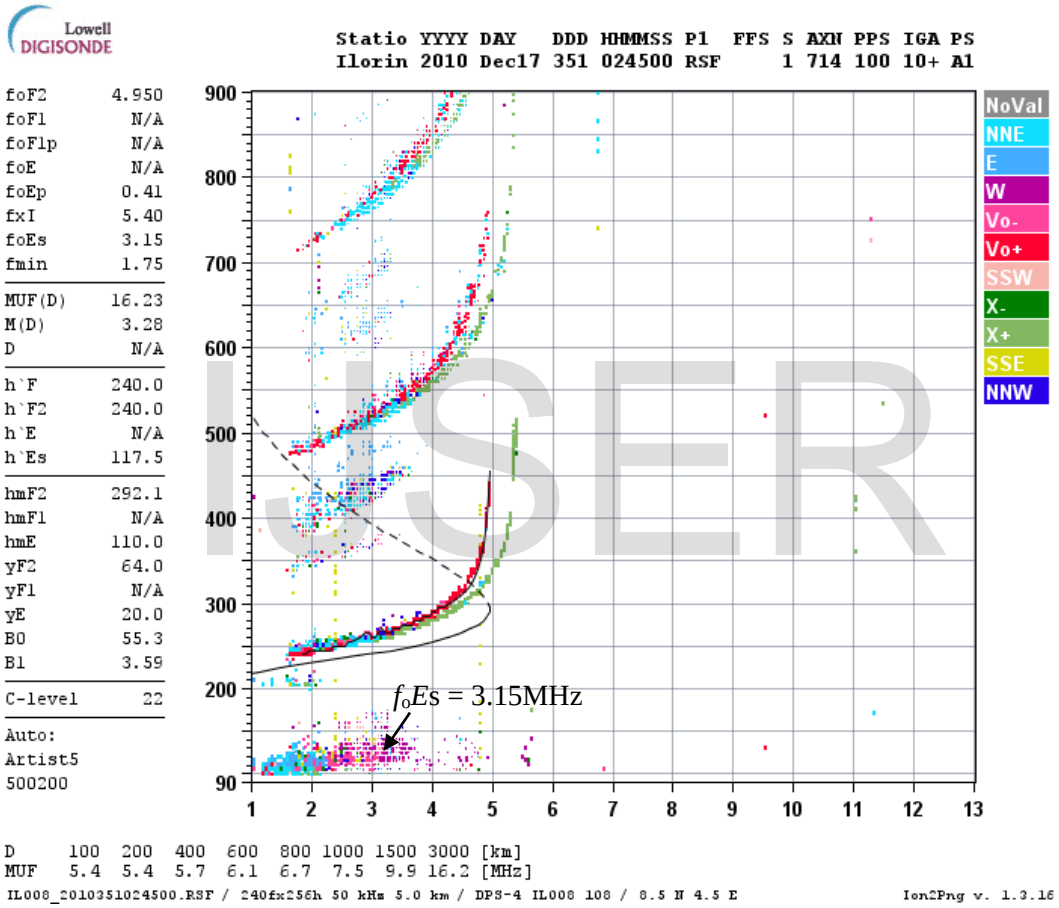

Fig 2.5: An example of typical sporadic E ionogram (Observatory, University of Ilorin on December 17, 2010 at Lat. 0.5°N, Long. 4.5°E).

2.6.3 IONOGRAM OF REGULAR E

The ionogram of a normal or regular E indicates that there is a significant transmission of signals in which there is a clear existence of a higher layer (F-layer). It shows distinct parameters as an indicator of E-layer. In this case, the value for f_oE =3.41MHz.

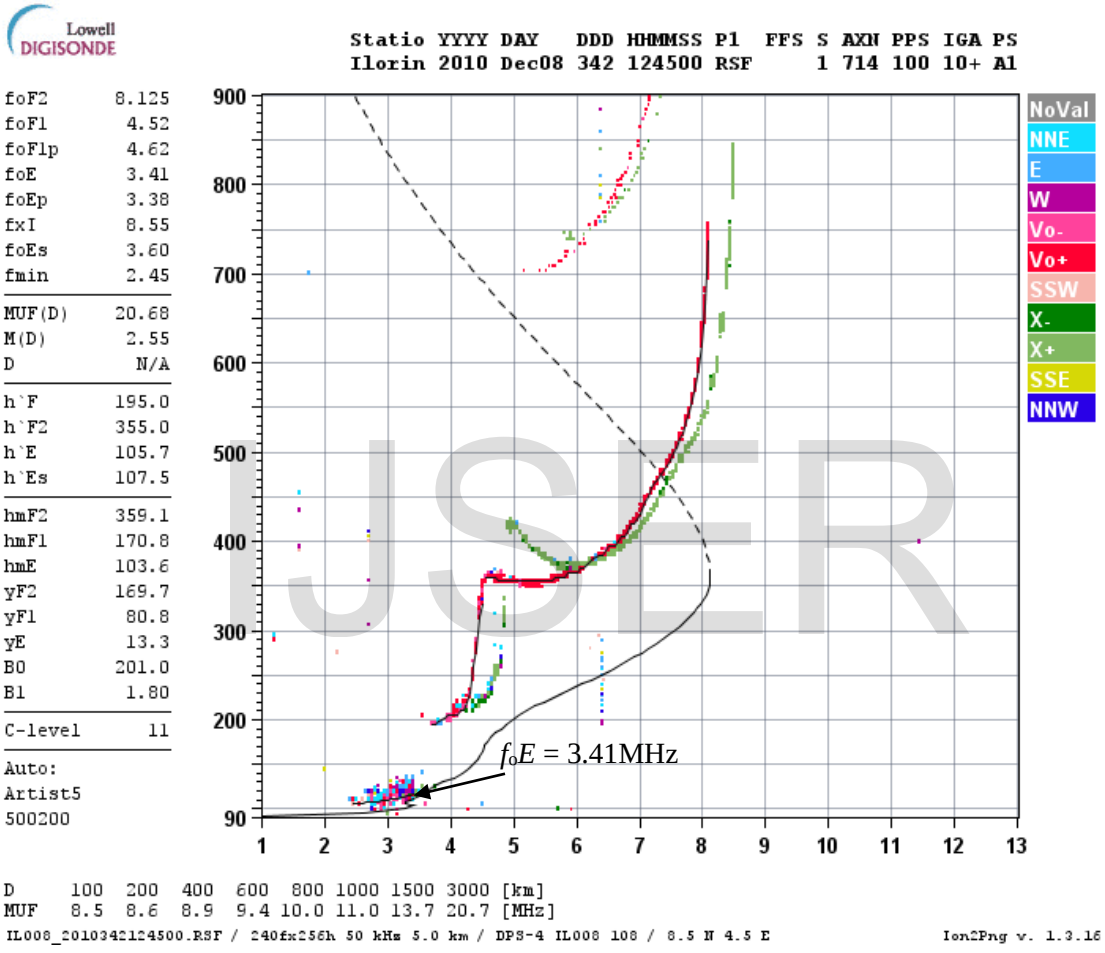

Fig 2.6: An example of typical regular E ionogram (Observatory, University of Ilorin on December 8, 2010 at Lat. 0.5°N, Long. 4.5°E).

For communication, the most important characteristic feature of the E region is the temporal and geographic variation of its critical frequency. In almost all other respects, the features of the E layer are very predictable compared with those of the F2 layer.

A large volume of vertical-incidence ionosonde data has been collected over about three solar cycles, and many features of the E region are therefore well known. The minimum virtual height of the E region and the variation of maximum electron density within this region as a function of time and geographic location are readily obtained from the ionograms. The phenomenology of sporadic-E has been investigated, but classification of sporadic-E types remains unresolved. The effects of different types of sporadic-E on oblique-incidence radio propagation are not established; as a result, the compilation of meaningful statistics to form the basis of predictions is difficult.

The E-region characteristics that have been systematically scaled from the vertical-incidence ionosonde records include:

f_oE	The critical frequency of the ordinary component of the E layer; i.e., that frequency at which the signal from the ionosonde just penetrates the E layer.
h_mE	The height of maximum ionization of the E layer, measured at the point where the trace of the next layer becomes visible.
h'*E*	The minimum virtual height of the E layer, measured at the point where the trace becomes horizontal.
f_oEs	The highest observed frequency of the ordinary component of sporadic-E (Es).
h'*E*s	The minimum virtual height of the sporadic-E layer, measured at the point where the trace becomes horizontal.
f_bEs	The blanketing frequency; i.e., the lowest ordinary wave frequency at which the Es layer begins to become transparent, usually determined from the

minimum frequency at which ordinary wave reflections of the first order are observed from a higher layer.

2.7 IONOSPHERIC MODEL

An ionospheric model is a mathematical description of the ionosphere as a function of location, altitude, day of year, phase of the sun spot cycle and geomagnetic activity. Geophysically, the state of the ionospheric plasma may be described by four parameters: electron density, electron and ion temperature and, since several species of ions are present, ionic composition (Gillard, *et. al.*, 1937). Radio propagation depends uniquely on electron density.

Models are usually expressed as computer programs. The model may be based on basic physics of the interactions of the ions and electrons with the neutral atmosphere and sun light, or it may be a statistical description based on a large number of observations or a combination of physics and observations.

One of the most widely used models is the International Reference Ionosphere (IRI) (IRI 2007), which is based on data and specifies the four parameters just mentioned (Bilitza, D. 2000). The IRI is an international project sponsored by the Committee on Space Research (COSPAR) and the International Union of Radio Science (URSI). The major data sources are the worldwide network of ionosondes, the powerful incoherent scatter radars (Jicamarca, Arecibo, Millstone Hill, Malvern, St. Santin), the ISIS and Alouette topside sounders, and in situ instruments on several satellites and rockets. IRI is updated yearly. IRI will be established in 2009 by the International Organization for Standardization (ISO) as standard TS16457. IRI is accurate in describing the variation of the electron density from bottom of the ionosphere to the altitude of maximum density than in describing the total electron content (TEC).

2.8 ANOMALIES TO THE IDEAL MODEL

Ionograms allow deducing not only the shape of the different layers but also the structure of the electron/ion-plasma. Rough traces, indicating non-homogeneity, are seen predominantly at night and at higher latitudes, and during disturbed conditions.

2.8.1 WINTER ANOMALY

At mid-latitudes, the F2 layer daytime ion production is higher in the summer, as expected, since the sun shines more directly on the earth. However, there are seasonal changes in the molecular-to-atomic ratio of the neutral atmosphere that cause the summer ion loss rate to be even higher.

The result is that the increase in the summertime loss overwhelms the increase in summertime production, and total F2 ionization is actually lower in the local summer months. This effect is known as the winter anomaly. The anomaly is always present in the northern hemisphere, but is usually absent in the southern hemisphere during periods of low solar activity.

2.8.2 EQUATORIAL ANOMALY

Fig. 2.7: Electric currents created in sunward ionosphere (Ionosphere - Wikipedia, the free encyclopedia.htm)

Within approximately ± 20 degrees of the magnetic equator, is the equatorial anomaly. It is the occurrence of a trough of concentrated ionization in the F2 layer. The Earth's magnetic field lines are horizontal at the magnetic equator. Solar heating and tidal oscillations in the lower ionosphere move plasma up and across the magnetic field lines.

This sets up a sheet of electric current in the E region which, with the horizontal magnetic field, forces ionization up into the F layer, concentrating at ± 20 degrees from the magnetic equator. This phenomenon is known as the equatorial fountain.

2.8.3 EQUATORIAL ELECTROJET

The worldwide solar-driven wind results in the so-called Sq (solar quiet) current system in the E region of the Earth's ionosphere (100–130 km altitude). Resulting from this current is an electrostatic field directed E-W (dawn-dusk) in the equatorial day side of the ionosphere. At the magnetic dip equator, where the geomagnetic field is horizontal, this electric field results in an enhanced eastward current flow within ± 3 degrees of the magnetic equator, known as the equatorial electrojet.

2.9 IONOSPHERIC PERTURBATIONS

1. X-RAYS: SUDDEN IONOSPHERIC DISTURBANCES (SID)

When the sun is active, strong solar flares can occur that will hit the Earth with hard X-rays on the sunlit side of the Earth. They will penetrate to the D-region, release electrons which will rapidly increase absorption causing a High Frequency (3-30 MHz) radio blackout. During this time Very Low Frequency (3 – 30 kHz) signals will become reflected by the D layer instead of the E layer, where the increased atmospheric density will usually increase the absorption of the wave, and thus dampen it (Hargreaves, 1992).

As soon as the X-rays end, the sudden ionospheric disturbance (SID) or radio black-out ends as the electrons in the D-region recombine rapidly and signal strengths return to normal.

2. PROTONS: POLAR CAP ABSORPTION (PCA)

Associated with solar flares is a release of high-energy protons. These particles can hit the Earth within 15 minutes to 2 hours of the solar flare. The protons spiral around and down the magnetic field lines of the Earth and penetrate into the atmosphere near the magnetic poles increasing the ionization of the D and E layers. PCA's typically last anywhere from about an hour to several days, with an average of around 24 to 36 hours (Blelly, 2007).

3. GEOMAGNETIC STORMS

A geomagnetic storm is a temporary intense disturbance of the Earth's magnetosphere. During a geomagnetic storm the F2 layer will become unstable, fragment, and may even disappear completely. In the Northern and Southern pole regions of the Earth aurora will be observable in the sky.

4. LIGHTNING

Lightning can cause ionospheric perturbations in the D-region in one of two ways. The first is through VLF frequency radio waves launched into the magnetosphere. These so-called "whistler" mode waves can interact with radiation belt particles and cause them to precipitate onto the ionosphere, adding ionization to the D-region. These disturbances are called Lightning-induced Electron Precipitation (LEP) events.

Additional ionization can also occur from direct heating/ionization as a result of huge motions of charge in lightning strikes. These events are called Early/Fast.

In 1925, C. F. Wilson proposed a mechanism by which electrical discharge from lightning storms could propagate upwards from clouds to the ionosphere. Around the same time, Robert Watson-Watt, working at the Radio Research Station in Slough, UK, suggested that the ionospheric sporadic E layer (Es) appeared to be enhanced as a result of lightning but that more work was needed. In 2005, C. Davis and C. Johnson, working at the Rutherford Appleton Laboratory in Oxfordshire, UK, demonstrated that the Es

layer was indeed enhanced as a result of lightning activity. Their subsequent research has focused on the mechanism by which this process can occur.

2.10 RADIO APPLICATION

DX communication, popular among amateur radio enthusiasts, is a term given to communication over great distances. Thanks to the property of ionized atmospheric gases to refract high frequency (HF, or shortwave) radio waves, the ionosphere can be utilized to "bounce" a transmitted signal down to ground. Transcontinental HF-connections rely on up to 5 bounces, or hops. Such communications played an important role during World War II. Karl Rawer's most sophisticated prediction method took account of several (zig-zag) paths, attenuation in the D-region and predicted the 11-years solar cycle by a method due to Wolfgang Gleißberg (John, 1995).

2.11 MECHANISM OF REFRACTION

When a radio wave reaches the ionosphere, the electric field in the wave forces the electrons in the ionosphere into oscillation at the same frequency as the radio wave. Some of the radio-frequency energy is given up to this resonant oscillation. The oscillating electrons will then either be lost to recombination or will re-radiate the original wave energy. Total refraction can occur when the collision frequency of the ionosphere is less than the radio frequency, and if the electron density in the ionosphere is great enough.

The critical frequency is the limiting frequency at or below which a radio wave is reflected by an ionospheric layer at vertical incidence. If the transmitted frequency is higher than the plasma frequency of the ionosphere, then the electrons cannot respond fast enough, and they are not able to re-radiate the signal.

It is calculated as shown below:

$$f_{critical} = 9 \times 10^{-3}\sqrt{N}$$

where N = electron density per cm3 and $f_{critical}$ is in MHz.

The Maximum Usable Frequency (MUF) is defined as the upper frequency limit that can be used for transmission between two points at a specified time.

where $f_{muf} = \frac{f_{critical}}{\sin \alpha}$ α = angle of attack, the angle of the wave relative to the horizon, and sin is the sine function.

The cut-off frequency is the frequency below which a radio wave fails to penetrate a layer of the ionosphere at the incidence angle required for transmission between two specified points by refraction from the layer (Grotz, 2007 and Jacobs, *et. al.*, 1995)).

2.12 OTHER APPLICATIONS

The open system electrodynamic tether, which uses the ionosphere, is being researched. The space tether uses plasma contactors and the ionosphere as parts of a circuit to extract energy from the Earth's magnetic field by electromagnetic induction.

CHAPTER THREE

ANALYSIS OF DATA

3.0 DATA AND METHOD OF ANALYSIS

The data used for this study are those obtained from Ionospheric Station at the University of Ilorin, Ilorin, (geographic 8.53°N latitude, 4.57°E longitude and dip 4.1°S) (Adeniyi, *et. al.*, 2009) using the Digisonde Portable Sounder DPS4.

Auto-scaled ionograms for the year 2010 were used. The E-layer parameters namely f_oE, h_mE, h`E, $f_oE$s and $h$`Es were the data extracted from the ionograms. The equipment is designed to measure its parameters at universal time (UT), hence the local time (LT) of Ilorin will be +1.

Between 21 and 28 days of data were selected for the months March/April (representing March Equinox), June (representing June Solstice), September (representing September Equinox) and December (representing December Solstice) (See Table 3.1)

Table 3.1: Number of observed days

OBSERVED MONTHS	OBSERVED NUMBER OF DAYS
March-April	21
June	21
September	28
December	23

The parameters f_oE, h_mE and $h`E$ for the normal E were obtained between 0600UT – 1800UT since the sunset time frequencies of the layer are usually too low for the digisonde to detect while the parameters $f_oEs$ and $h`Es$, for sporadic E were observed during the hours of 0000UT – 2300UT.

The daily and monthly mean of frequencies and heights were calculated in order to show their variations. A scattered XY graph was plotted for all the hourly values of the frequency f_oE in which a straight line showed the monthly mean. A line graph was plotted for the values of f_oEs, $h`Es$, $h_mE$ and $h`E$ representing their monthly mean.

CHAPTER FOUR

OBSERVATIONS AND RESULTS

4.0 RESULTS

CRITICAL FREQUENCY f_oE

The diurnal variation and monthly mean of the frequencies f_oE for the four seasons are shown in Fig. 4.1

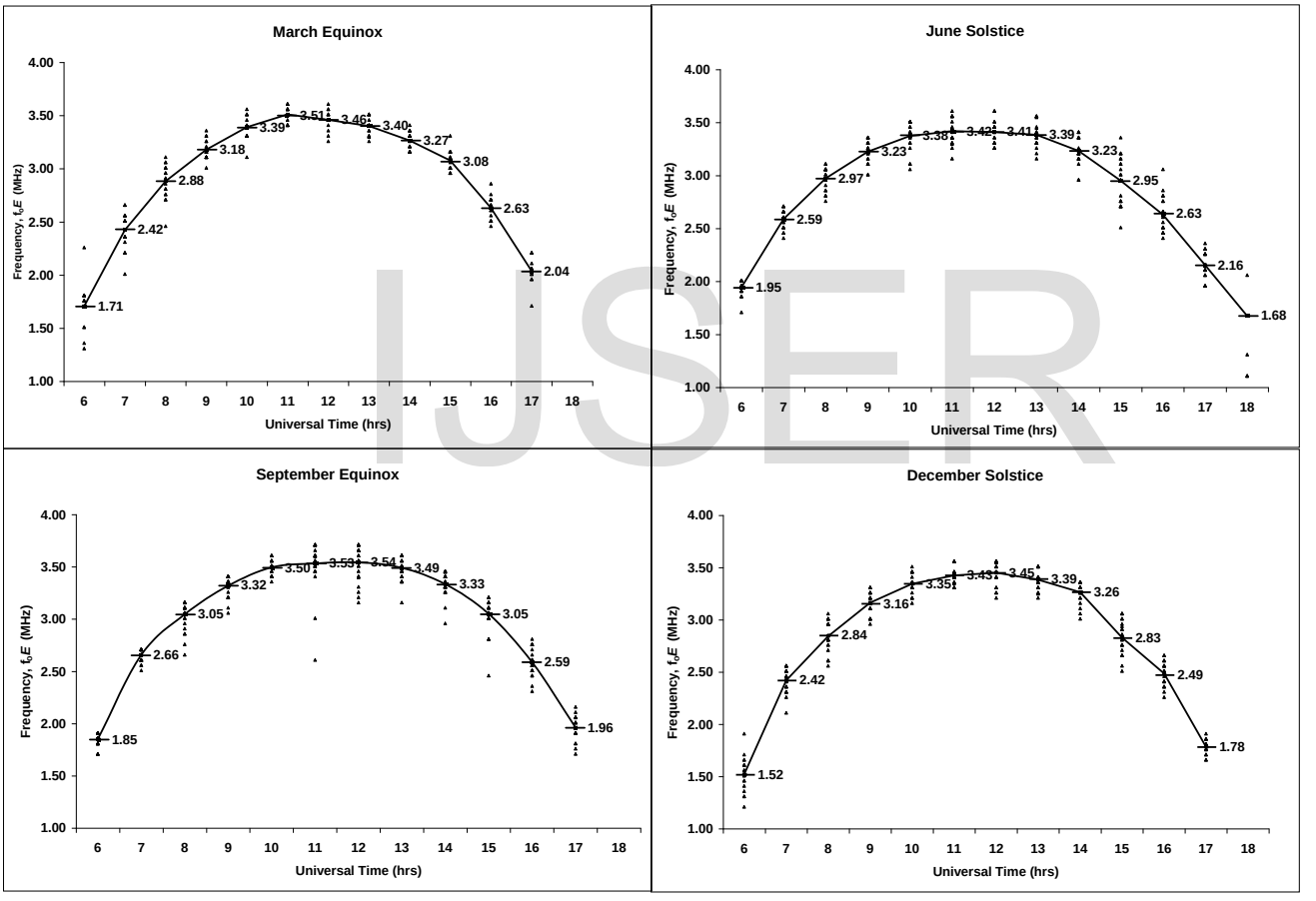

Fig.4.1: Mean diurnal variation of the critical frequency of regular *E* for the four seasons of the year.

MARCH EQUINOX

For the March equinox, the frequencies of normal E-layer begin to rise from 0600UT and attain its maximum/peak around 1100UT. Thereafter, f_oE gradually decreases attaining its minimum at about 1700UT. The sunrise minimum is 1.71MHz. The peak of f_oE for this season is 3.51MHz. The sunset time minimum value for this season is 2.04MHz.

JUNE SOLSTICE

For the June solstice, the frequencies of normal E-layer begin to rise from 0600UT and attain its maximum/peak around 1300UT. Thereafter, f_oE gradually decreases attaining its minimum at about 1800UT. The sunrise minimum is 1.95MHz. The peak of f_oE for this season is 3.39MHz. The sunset time minimum value for this season is 1.68MHz.

SEPTEMBER EQUINOX

For the September equinox, the frequencies of normal E-layer begin to rise from 0600UT and attain its maximum/peak around 1200UT. Thereafter, f_oE gradually decreases attaining its minimum at about 1700UT. The sunrise minimum is 1.85MHz. The peak of f_oE for this season is 3.54MHz. The sunset time minimum value for this season is 1.96MHz.

DECEMBER SOLSTICE

For the December solstice, the frequencies of normal E-layer begin to rise from 0600UT and attain its maximum/peak around 1200UT. Thereafter, f_oE gradually decreases attaining its minimum at about 1700UT. The sunrise minimum is 1.52MHz. The peak of f_oE for this season is 3.45MHz. The sunset time minimum value for this season is 1.78MHz.

SEASONAL EFFECT

The seasonal behaviour of normal E-layer can be summarized as shown Fig. 4.2

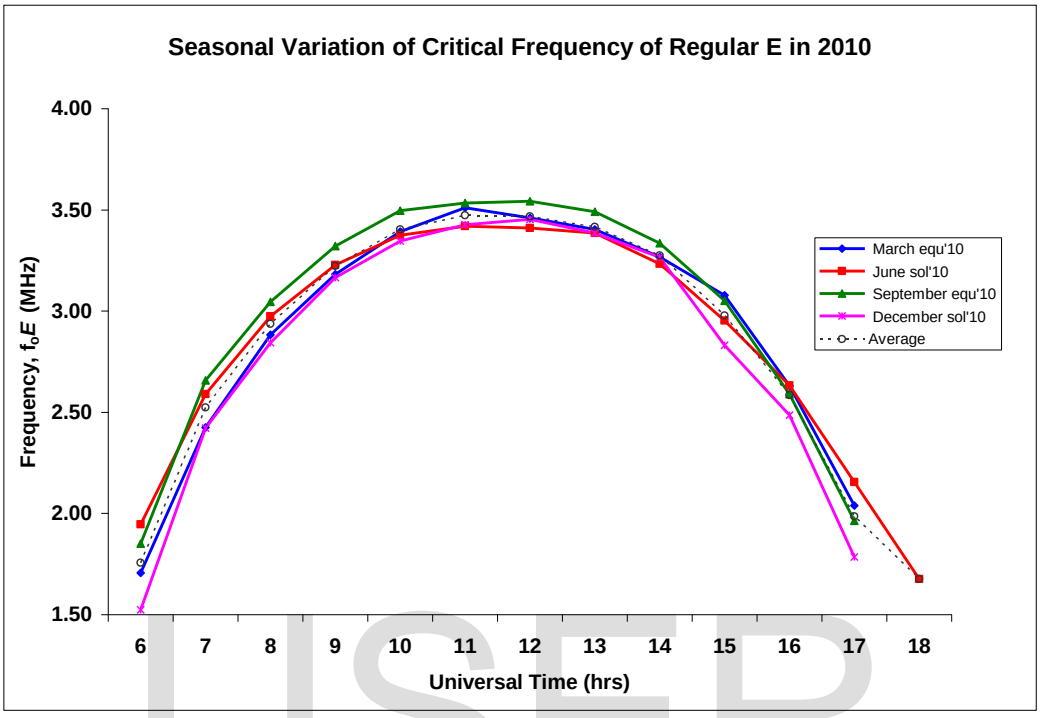

Fig. 4.2: Seasonal Variation of the critical frequency of regular E layer for the year 2010

The result shows that the September equinox shows the highest peak value of 3.54MHz at 1200UT. The seasonal features that were observed are the equinox months having the same frequency before attaining their peak value; the solstice months having same frequency before and after attaining their peak and the sunset time minimum value for which the solstice months give a lower value than the equinox months.

It is also observed that all the plots have similar pattern of graph which obeys Chapman's law of ionization. The E-layer appeared at 0600UT and disappeared at 1700UT in all the seasons except in June solstice where it extended to 1800UT.

CRITICAL FREQUENCY f_oEs

The diurnal variation and monthly mean of the frequencies of sporadic E, f_oEs for the four seasons are shown in Fig. 4.3

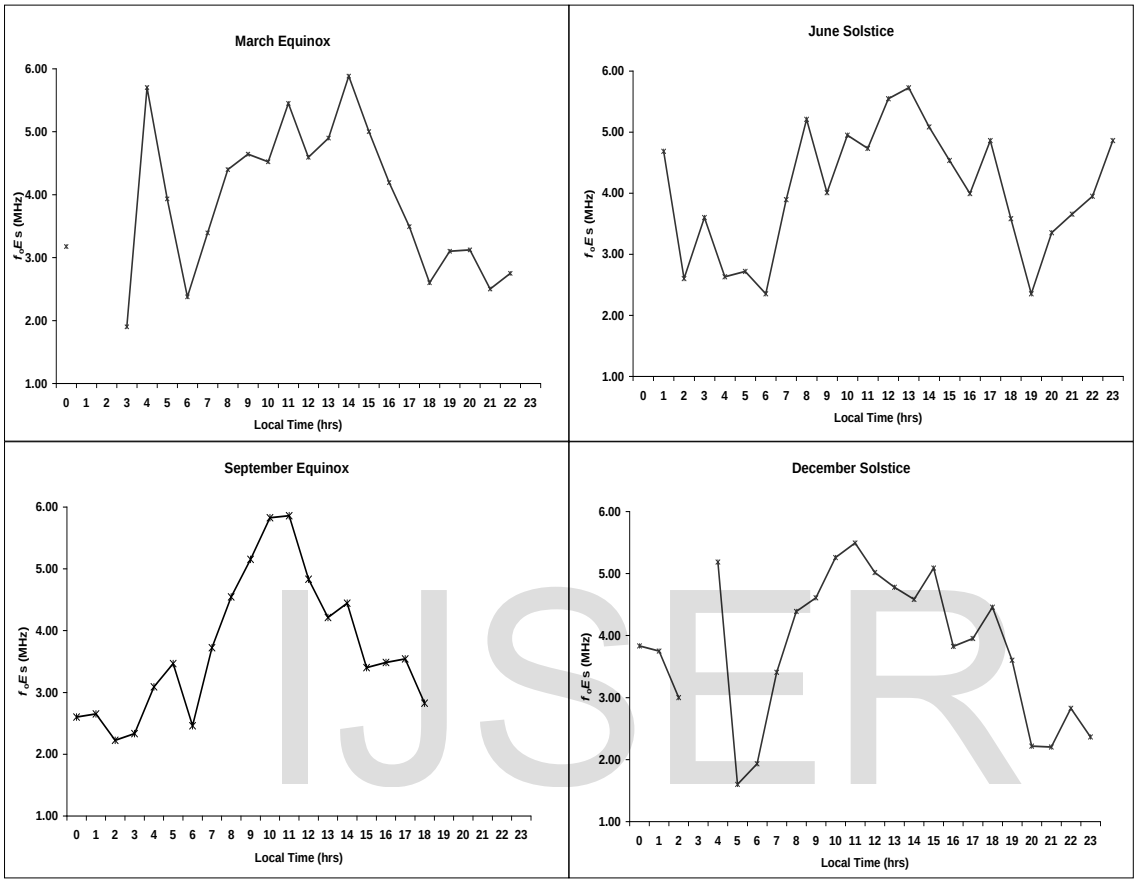

Fig. 4.3: Mean diurnal variation of the critical frequencies of sporadic *E* for the four seasons of the year.

MARCH EQUINOX

For March equinox, the sporadic E was present all through the season except at 0100UT and 2300UT. In this season, f_oEs was seen to have a frequency as low as 1.90MHz at 0300UT and as high as 5.88MHz at 1400UT.

JUNE SOLSTICE

For June solstice, the sporadic E was present all through the season except at 0000UT. The frequency of sporadic E, f_oEs was seen to have a frequency as high as 5.73MHz at 1300UT and as low as 2.35MHz at 0600UT and 1900UT.

SEPTEMBER EQUINOX

For September equinox, the sporadic E was not present all through the season. It was seen between 0000UT and 1800UT. The sporadic E was seen to have a peak frequency, f_oEs of 5.86MHz at 1100UT and a low value of 2.23MHz at 0200UT.

DECEMBER SOLSTICE

For December solstice, the sporadic E was present all through the season except at 0300UT. The sporadic E was seen to have a peak frequency of 5.49MHz at 1100UT and a low value of 1.60MHz at 0500UT.

SEASONAL EFFECT

The seasonal behaviour of sporadic E-layer can be summarized as shown Fig. 4.4

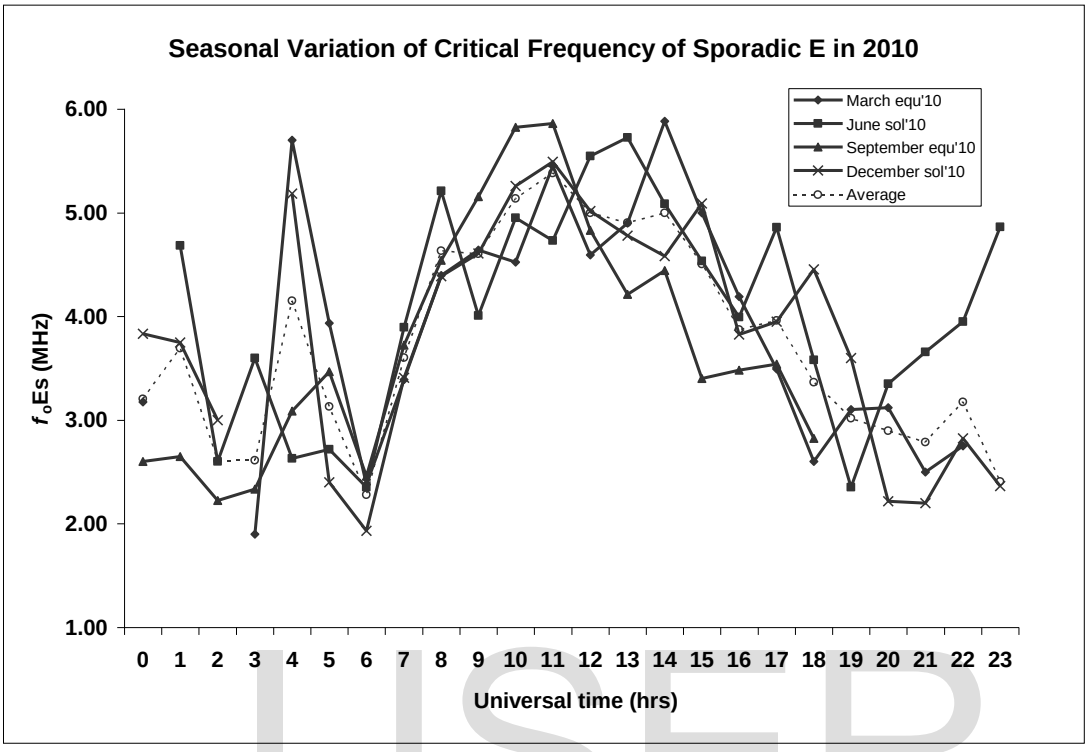

Fig. 4.4: Seasonal Variation of critical frequency of sporadic E layer for the four seasons

The seasonal pattern that can be observed is its undulating feature or instability. Also, the observable seasonal effects are; at 0600UT during the equinox, the f_oEs were the same and during the solstice, the f_oEs extends to 2300UT. The sporadic E attained its peak frequency at 5.88MHz at 1400UT during the March equinox and had its lowest value of 1.60MHz at 0500UT during the December solstice.

HEIGHTS OF NORMAL E (h_mE and $h`E$)

The monthly mean of the heights h_mE and $h`E$ for the four seasonal months is shown in Fig. 4.5

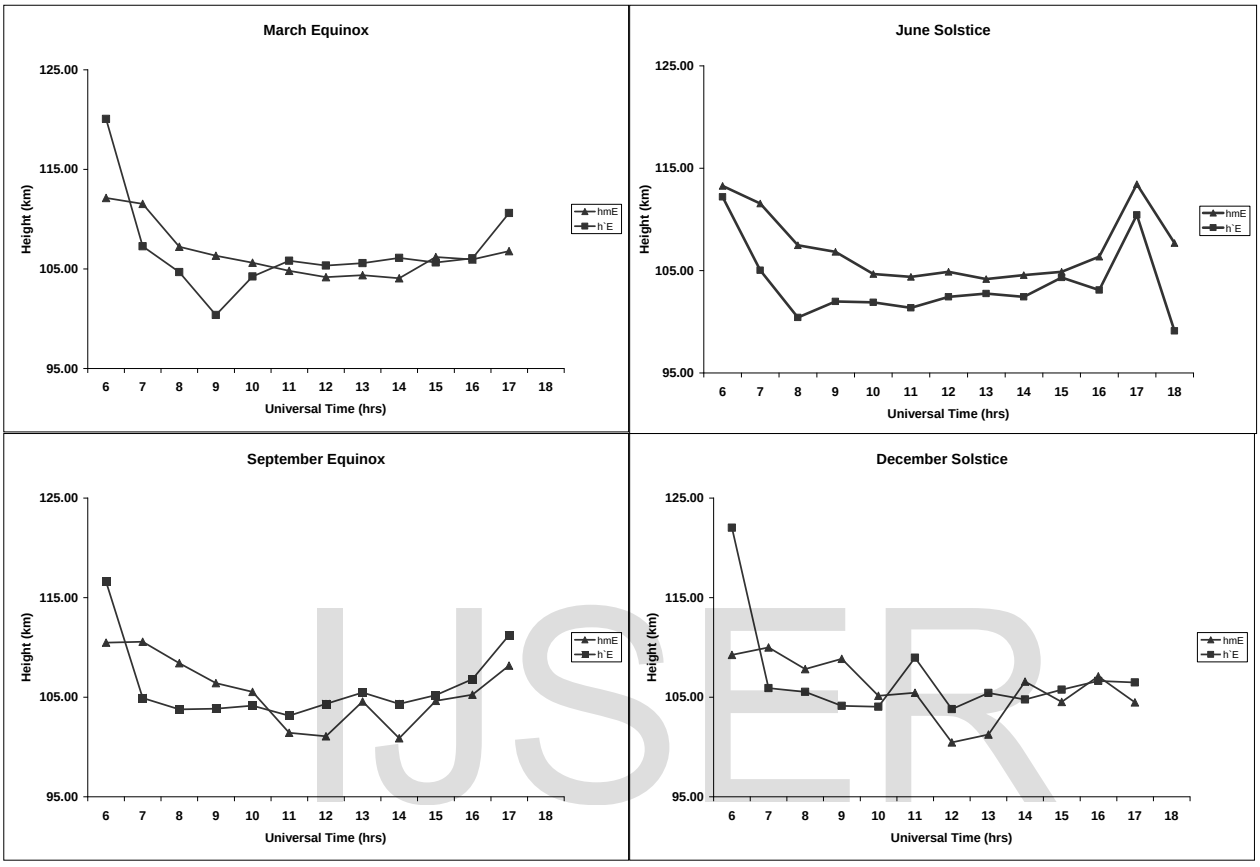

Fig. 4.5: Mean diurnal variation of h_mE and $h`E$ for the four seasons of the year.

MARCH EQUINOX

During this season, it can be observed that at sunrise time, the h_mE had a higher value which reduces during noontime and then rises to a high value during the sunset time. For the $h`E$, its value was high during sunrise time, reduces before noontime and then rises to a relatively constant value till the sunset time. At 0600UT, the average maximum true height ($h_mE$ ) of ionization of regular E was 112.13km and its virtual component ($h`E$) was 120.05km and then reduced to 110.61km and 106.98km respectively at 1700UT. The lowest value of h_mE was observed to be 104.06km at 1400UT and that of $h`E$ was 100.37km at 0900UT.

JUNE SOLSTICE

It can be observed that at 0600UT, the average maximum true height (h_mE) of ionization of regular E was 113.27km and its virtual component ($h`E$) was 112.19km and then reduced to 107.68km and 99.10km respectively at 1800UT. The lowest value of $h_mE$ was observed to be 104.17km at 1300UT and that of $h`E$ was 99.10km at 1800UT.

SEPTEMBER EQUINOX

It can be observed that at 0600hrs, the average maximum true height (h_mE) of ionization of regular E was 110.48km and its virtual component ($h`E$) was 116.57km and then reduced to 108.16km and 111.21km respectively at 1700UT. The lowest value of $h_mE$ was observed to be 100.87km at 1400UT and that of $h`E$ was 103.14km at 1100UT.

DECEMBER SOLSTICE

It can be observed that at 0600UT, the average maximum true height (h_mE) of ionization of regular E was 109.25km and its virtual component ($h`E$) was 112.01km and then reduced to 104.46km and 106.46km respectively at 1700UT. The lowest value of $h_mE$ was observed to be 100.45km and that of $h`E$ was 103.78km, both at 1200UT.

General Observations

In all the seasons, the seasonal pattern could describe as follows that at sunrise time, the h_mE had a higher value which reduces during noontime and then rises to a high value during the sunset time. For the

h`E*, its value was high during sunrise time, reduces before noontime and then rises to a relatively constant value till the sunset time. It is also observed that the values of *h`E was higher than that of h_mE at sunrise time of 0600UT and sunset time of 1700UT in all the seasons except in June where it was the reverse at 1700UT.

HEIGHTS OF SPORADIC E (*h`Es*)

The monthly mean of the heights *h`Es* for the four seasonal months is shown in Fig. 4.6

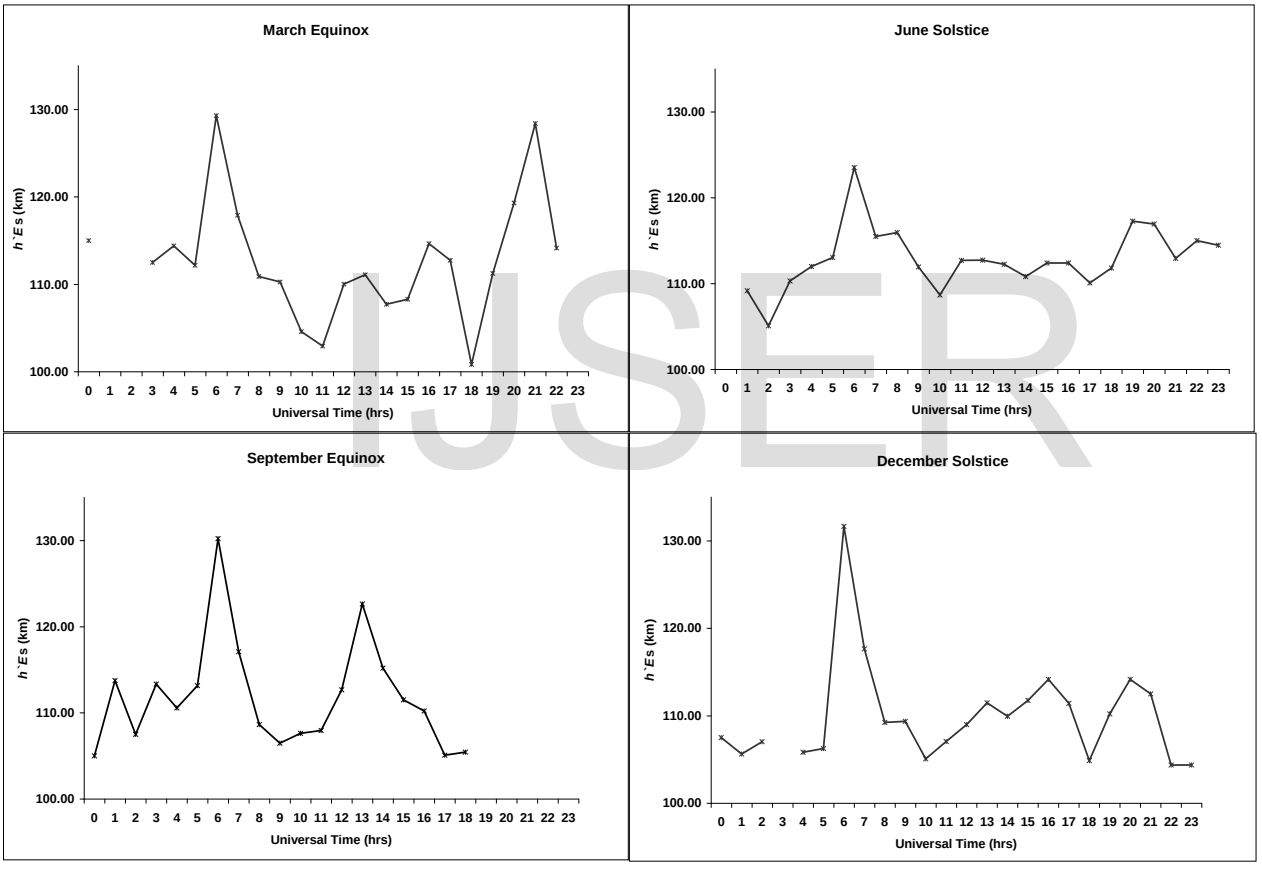

Fig. 4.6: Mean diurnal variation of *h`Es* for the four seasons of the year.

MARCH EQUINOX

In this season, the undulating pattern of *h`Es* can be observed. It had its peak value of 129.29km at 0600UT and its lowest value of 100.83km at 1800UT.

JUNE SOLSTICE

The pattern in this season is an undulating type as well. It can be observed also that the virtual height (*h`Es*) of sporadic E had its peak value of 123.52km at 0600UT and its lowest value of 105.07km at 0200UT.

SEPTEMBER EQUINOX

During this season, the undulating pattern was also observable. It can be observed also that the virtual height (*h`Es*) of sporadic E had its peak value of 130.22km at 0600UT and its lowest value of 105.00km at 0000UT.

DECEMBER SOLSTICE

In this season, the undulating pattern can be observed. Also, the virtual height (*h`Es*) of sporadic E had its peak value of 131.65km at 0600UT and its lowest value of 104.38km at 2300UT.

General Observations

It can be observed also that the virtual height (*h`Es*) of sporadic E occurred at some undulating high and low altitudes as usual in all the season and there were some disappearances in March equinox and December solstice.

Figures 4.7 – 4.9 show the seasonal plots of h_mE, $h`E$, and $h`Es$ against local time for seasons respectively.

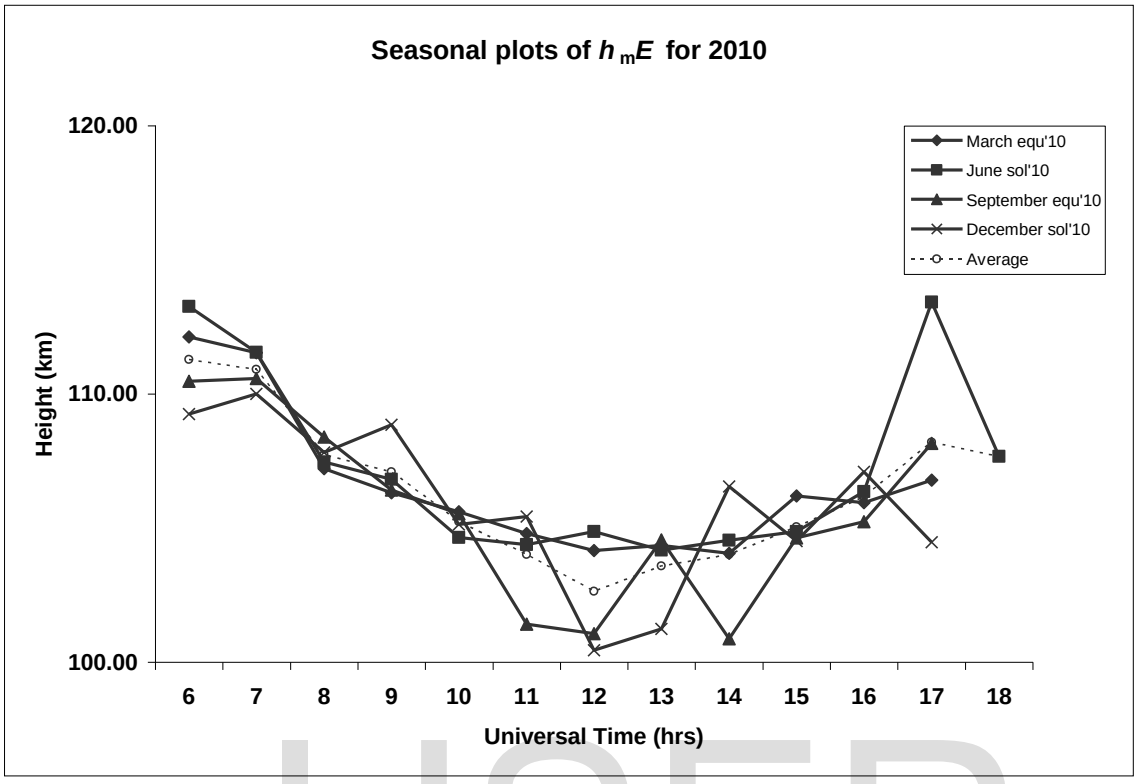

Fig. 4.7: Seasonal Variation of h_mE for the four seasons

The seasonal pattern of the maximum true height of ionization of the regular E was observed to be high during sunrise time, reduced during noon time and then ascended thereafter till sunset time. The only observable seasonal effect was that during the equinox, the heights did not exceed 1700UT. During this season, the peak height of 113.43km was attained at 1700UT in the June solstice while the lowest value was 100.45km at 1200UT in the December solstice as shown in Fig. 4.7 above.

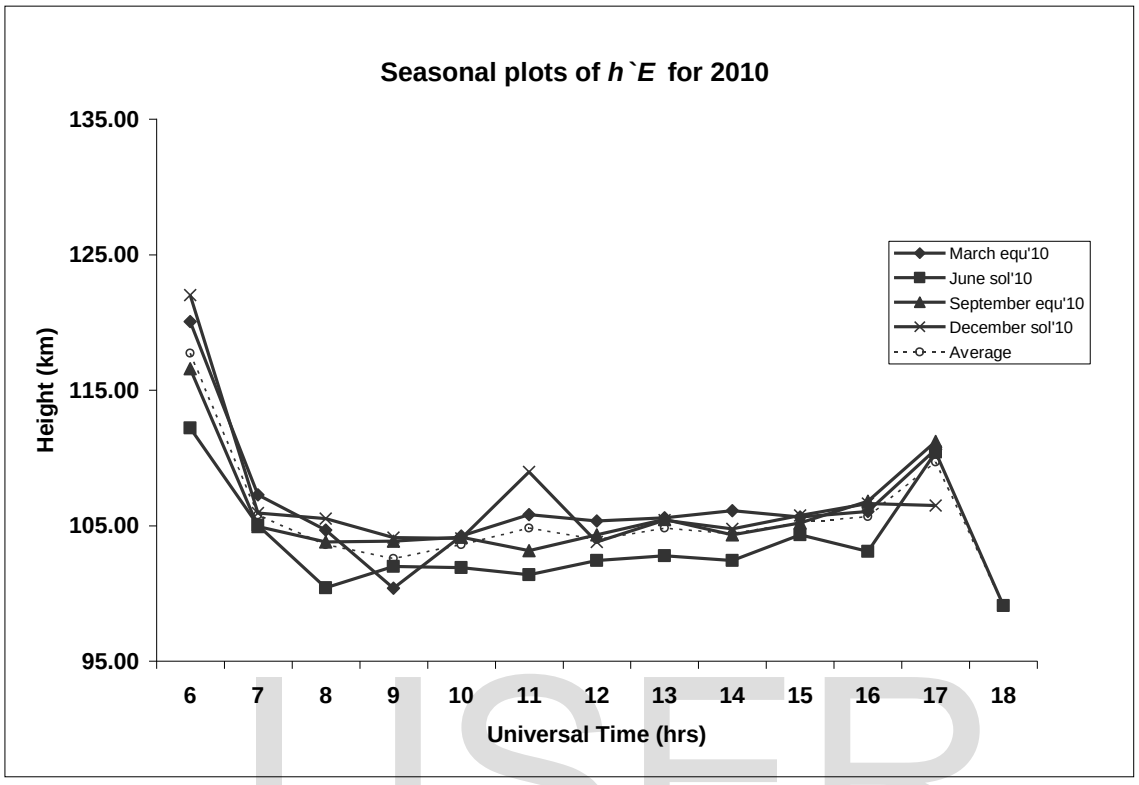

Fig. 4.8: Seasonal Variation of *h`E* for the four seasons

The seasonal pattern of virtual height of the regular E (*h`E)* was observed to have high values at the sunrise time, reduces before noon time and then remain relatively constant till the sunset time all through the equinoxes and solstices as well. The observable seasonal effect was that at 1000UT and at 1300UT, the heights were the same during the equinox. The peak value for the four seasons was 112.01km at 0600UT which occurred in the December solstice while the lowest value of 99.10km at 1800UT occurred in June solstice as shown in Fig. 4.8 above.

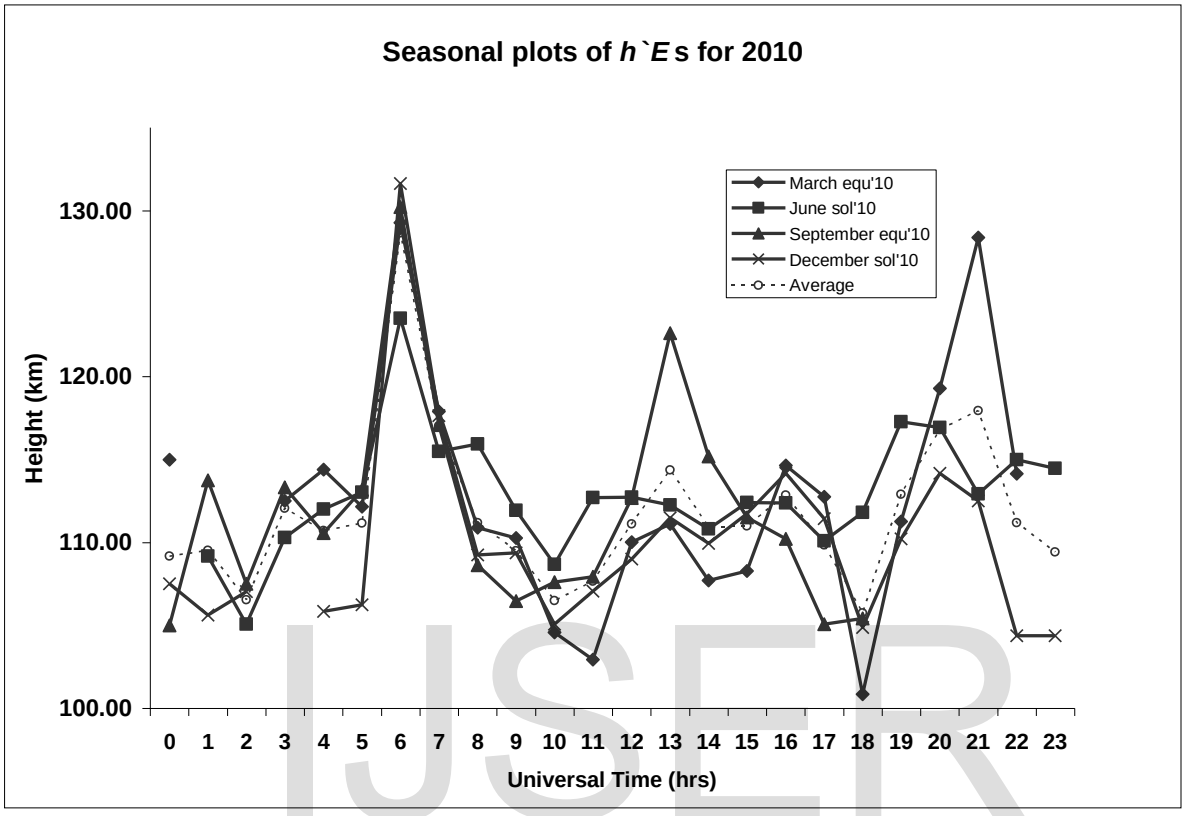

Fig. 4.9: Seasonal Variation of *h`Es* in 2010

The virtual heights of sporadic E (*h`Es*) was observed to be unstable all through the equinoxes and solstices. The observable seasonal effects are during the equinox, equal heights were attained at 0600UT and the heights, though of different values, were sustained till 2300UT in the solstices. The lowest value in the four seasons was 100.83km at 1800UT which occurred in the March equinox while the peak value of 131.65km at 0600UT occurred in the December solstice as shown in Fig. 4.9 above.

4.1 STANDARD DEVIATION

Tables 4.1- 4.4 show the hourly averages and the standard deviations for the h_mE and $h`E$ for the days investigated as well as the number of days used in computing these averages.

Table 4.1: Mean heights h_mE and $h`E$ for March equinox 2010

UT	No. of Days	h_mE (km)	Std. Dev. for h_mE (km)	$h`E$ (km)	Std. Dev. for $h`E$ (km)
6	13	112.13	0.43	120.05	9.05
7	17	111.53	3.05	107.25	1.83
8	18	107.21	0.63	104.66	3.04
9	17	106.32	0.50	100.37	2.73
10	11	105.61	0.57	104.23	1.12
11	15	104.80	0.45	105.81	0.34
12	14	104.16	0.14	105.34	0.17
13	13	104.35	0.21	105.57	0.38
14	16	104.06	1.50	106.11	0.33
15	17	106.19	0.17	105.64	0.29
16	17	105.95	0.59	106.05	3.22
17	16	106.78	-	110.61	-

The h_mE was observed to have a standard deviation ranging from 0.14km to 3.05km while for $h`E$, the range was 0.17km to 9.05km.

Table 4.2: Mean heights h_mE and $h`E$ for June solstice 2010

UT	No. of Days	h_mE (km)	Std. Dev. for h_mE (km)	$h`E$ (km)	Std. Dev. for $h`E$ (km)
6	20	113.27	1.21	112.19	5.07
7	17	111.55	2.89	105.02	3.26
8	19	107.46	0.46	100.42	1.10
9	21	106.82	1.53	101.97	0.05
10	20	104.65	0.20	101.89	0.38
11	19	104.37	0.35	101.35	0.76
12	20	104.87	0.49	102.43	0.23
13	18	104.17	0.27	102.76	0.23
14	20	104.55	0.22	102.43	1.34
15	21	104.86	1.06	104.31	0.86
16	21	106.36	4.99	103.10	5.18
17	21	113.43	4.07	110.43	8.01
18	4	107.68	-	99.10	-

The h_mE was observed to have a standard deviation ranging from 0.20km to 4.99km while for $h`E$, the range was 0.05km to 8.01km.

Table 4.3: Mean heights h_mE and $h`E$ for September equinox 2010

UT	No. of Days	h_mE (km)	Std. Dev. for h_mE (km)	$h`E$ (km)	Std. Dev. for $h`E$ (km)
6	28	110.48	0.07	116.57	8.24
7	28	110.57	1.54	104.92	0.81
8	28	108.40	1.40	103.78	0.05
9	26	106.41	0.62	103.84	0.21
10	25	105.54	2.91	104.14	0.71
11	27	101.42	0.25	103.14	0.84
12	27	101.06	2.47	104.32	0.80
13	26	104.56	2.61	105.45	0.80
14	26	100.87	2.66	104.32	0.62
15	25	104.62	0.43	105.19	1.14
16	26	105.23	2.07	106.81	3.12
17	22	108.16	-	111.21	-

The h_mE was observed to have a standard deviation ranging from 0.07km to 2.91km while for $h`E$, the range was 0.05km to 8.24km.

Table 4.4: Mean heights h_mE and $h`E$ for December solstice 2010

UT	No. of Days	h_mE (km)	Std. Dev. for h_mE (km)	$h`E$ (km)	Std. Dev. for $h`E$ (km)
6	20	109.25	0.53	122.01	11.38
7	23	110.00	1.54	105.91	0.28
8	23	107.82	0.73	105.52	0.99
9	22	108.85	2.64	104.12	0.06
10	22	105.13	0.22	104.04	3.47
11	21	105.43	3.53	108.95	3.65
12	22	100.45	0.56	103.78	1.15
13	23	101.24	3.75	105.41	0.46
14	23	106.55	1.44	104.76	0.69
15	23	104.51	1.83	105.74	0.63
16	23	107.10	1.86	106.63	0.12
17	21	104.46	-	106.46	-

The h_mE was observed to have a standard deviation ranging from 0.22km to 3.75km while for $h`E$, the range was 0.06km to 11.38km.

There were no seasonal correlation in the h_mE and $h`E$ of the regular E during equinoxes nor solstices. For the $h_mE$, the minimum value of the standard deviation is 0.07km in September equinox and its maximum is 3.75km in December solstice while for $h`E$, the minimum value of the standard deviation is 0.05km in June solstice and September equinox and its maximum is 11.38km in December solstice.

Table 4.5 - 4.8 shows the hourly averages and the standard deviations for the $h`Es$ for the days investigated as well as the number of days used in computing these averages.

Table 4.5: Mean heights *h`Es* for March equinox 2010

UT	No. of Days	*h`Es* (km)	Std. Dev. for *h`Es* (km)
0	2	115.00	81.32
1	0	0.00	0
2	0	0.00	79.55
3	1	112.50	1.34
4	1	114.40	1.58
5	3	112.17	12.11
6	13	129.29	8.06
7	10	117.90	4.96
8	12	110.88	0.44
9	11	110.25	4.01
10	11	104.58	1.17
11	9	102.92	5.01
12	8	110.01	0.77
13	9	111.10	2.40
14	6	107.70	0.41
15	5	108.28	4.50
16	5	114.64	1.34
17	7	112.74	8.42
18	5	100.83	7.37
19	3	112.25	5.69
20	2	119.30	6.43
21	1	128.40	10.08
22	2	114.15	-
23	0	-	-

The *h`Es* was observed to have a standard deviation ranging from 0.00km to 81.32km.

Table 4.6: Mean heights *h`Es* for June solstice 2010

UT	No. of Days	*h`Es* (km)	Std. Dev. for *h`Es* (km)
0	0	0.00	77.19
1	3	109.17	2.90
2	3	105.07	3.70
3	4	110.30	1.20
4	5	112.00	0.73
5	8	113.04	7.41
6	13	123.52	5.68
7	11	115.49	0.32
8	13	115.95	2.84
9	15	111.93	2.29
10	12	108.68	2.84
11	14	112.71	0.01
12	11	112.73	0.34
13	8	112.25	1.02
14	10	110.81	1.13
15	10	112.41	0.02
16	7	112.39	1.63
17	11	110.08	1.23
18	11	111.82	3.86
19	7	117.27	0.24
20	10	116.93	2.83
21	3	112.93	1.46
22	2	115.00	0.37
23	4	114.48	-

The *h`Es* was observed to have a standard deviation ranging from 0.01km to 77.19km.

Table 4.7: Mean heights *h`Es* for September equinox 2010

UT	No. of Days	*h`Es* (km)	Std. Dev. for *h`Es* (km)
0	1	105.00	6.19
1	2	113.75	4.42
2	2	107.50	4.12
3	3	113.33	1.95
4	4	110.58	1.83
5	6	113.17	12.06
6	27	130.22	9.29
7	18	117.08	5.98
8	23	108.63	1.53
9	24	106.47	0.81
10	18	107.61	0.23
11	16	107.94	3.35
12	14	112.67	7.04
13	8	122.63	5.25
14	8	115.20	2.60
15	6	111.52	0.92
16	9	110.21	3.63
17	6	105.08	0.24
18	4	105.43	-
19	0		
20	0		
21	0		
22	0		
23	0		

The *h`Es* was observed to have a standard deviation ranging from 0.23km to 12.06km.

Table 4.8: Mean heights *h`Es* for December solstice 2010

UT	No. of Days	*h`Es* (km)	Std. Dev. for *h`Es* (km)
0	3	107.50	1.33
1	4	105.63	0.99
2	4	107.03	75.68
3	0	0.00	74.84
4	3	105.83	0.29
5	3	106.25	17.96
6	14	131.65	9.90
7	14	117.65	5.94
8	13	109.25	0.09
9	19	109.37	3.04
10	19	105.07	1.40
11	20	107.06	1.37
12	16	108.99	1.77
13	14	111.49	1.09
14	12	109.94	1.27
15	9	111.74	1.71
16	12	114.17	1.94
17	14	111.43	4.63
18	10	104.88	3.77
19	8	110.21	2.80
20	3	114.17	1.18
21	1	112.50	5.75
22	4	104.38	0.00
23	4	104.38	-

The *h`Es* was observed to have a standard deviation ranging from 0.00km to 75.68km.

During the solstices, the maximum values of the standard deviation of $h`E$ of the sporadic E were very close. The minimum value of the standard deviation of $h`E$ is 0.00km in March equinox and December solstice and its maximum is 81.32km in March solstice.

4.3 PERCENTAGE FREQUENCY OF OCCURRENCE OF SPORADIC E

The percentage frequency of occurrence of sporadic E is summarised as shown in Table 4.9.

Table 4.9: Number of occurrences of sporadic E-layer for the four seasons

	Number of Observed Occurrences of Sporadic E				**Total**
	March	June	September	December	
Sporadic E	126	196	199	223	**744**

Total Number of Observed Occurrences (ionograms) = 744

Percentage of occurrence of sporadic E in March equinox = $\frac{126}{744}\times 100$

= 17%

Percentage of occurrence of sporadic E in June solstice = $\frac{196}{744}\times 100$

= 26%

Percentage of occurrence of regular E in September equinox = = $\frac{199}{744}\times 100$

$= \quad 27\%$

Percentage of occurrence of sporadic E in December solstice $= \frac{223}{744} \times 100$

$= 30\%$

It can be observed that the seasons, the March equinox had the lowest occurrence of sporadic E of 17% while the December solstice had the highest occurrence of sporadic E of 30%.

4.4 OCCURRENCE FREQUENCY OF SPORADIC E

The occurrence frequency of sporadic E for the four seasons are summarised as shown in Fig. 4.10.

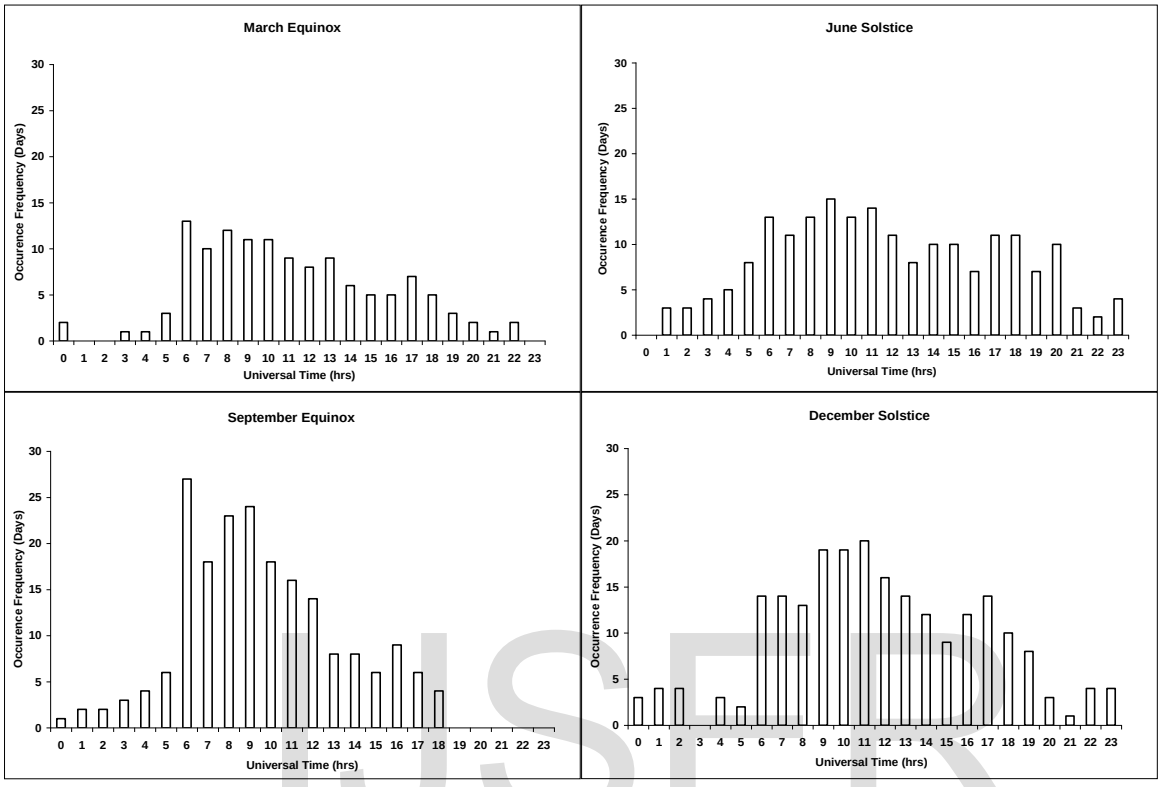

Fig. 4.10: The occurrence frequency of sporadic E for the four seasons

During the four seasons, it can be observed that the days in which the sporadic E occurred were consistent high in June solstice and low in March equinox. Also, it occurred between 0000UT and 2300UT in all the seasons except in September equinox where it was truncated at 1800UT, in March equinox it truncated between 0100UT and 0200UT; in June solstice at 0000UT and in December solstice at 0300UT. This is useful guide for amateur radio or TV stations.

CHAPTER FIVE

DISCUSSION AND CONCLUSIONS

The regular E-layer was noticeable from 0600UT to 1800UT in the June Solstice, while in March Equinox, September Equinox and December Solstice, it faded out at 1700UT. But the traces of sporadic E were found to be present both in the day time and the night time.

On the average, the frequencies of sporadic E (f_oEs) were found to be higher than that of regular E (f_oE). It was showed that during the equinoxes and solstices, the regular E became noticeable at a sunrise minimum frequency of 1.52MHz at 0600UT, attains its peak value of 3.54MHz at noon time 1200UT and then became unnoticeable at sunset time minimum frequency of 1.68MHz at 1800UT whereas for the sporadic E, its frequency f_oEs was 2.60MHz at 0000UT, 5.88MHz at 1400UT and 2.86MHz at 2300UT.

The peak heights of sporadic E ($h`Es$) are also higher than that of regular E ($h_mE$ and $h`E$) as it can be seen during the four seasons that sporadic E was found to have attained a height of 128.67km, while that of the regular E was 111.28km on the average.

The values of the frequencies and heights obtained as stated above can be used as a guide for the setting up of amateur radio or TV stations. The plots of average f_oE and f_oEs show that while the f_oE increases from the sunrise time, obtains its peak at the noon time and disappears at sunset time, being steadily stable; the f_oEs undulates with various high and low altitudes, proving its instability since its occurrence is short-lived.

In conclusion, in the year 2010, the behaviour of the E-layer in Ilorin was found to similar to the existing features in other equatorial locations in that it appears as early as 0000UT sporadically and becomes normal or regular at the sunrise time of about 0600UT, attains its peak at the noon time between 1100UT and 1200UT and thereafter disappears normally at the sunset time of about 1700UT but not sporadically, as it drifts into the night time till 2300UT.

REFERENCES

Adeniyi, J.O., et al (2009) Analysis on 29 March 2006 eclipse effect on the ionosphere over Ilorin, Nigeria, J. Geophys. Res., 114, A11303, doi:10.1029/2009JA014416 www.agu.org/pubs/crossref/2009/2009JA014416.shtml

Appleton, E. V. (1931) "The Timing of Wireless Echoes, the use of television and picture transmission", Wireless World, 14, January 1931, pp. 43-44

Bilitza, D. (2001) International Reference Ionosphere 2000.Radio Sci.36,#2,261-275 2001 http://ccmc.gsfc.nasa.gov/modelweb/ionos/iri.html http://www.swpc.noaa.gov/forecast_verification/F10.html

Blelly, P.L., et al (2007) Handbook of the Solar-Terrestrial Environment, Springer-Verlag Berlin Heidelberg, pp. 189-220, 2007. DOI: 10.1007/11367758_8

Breit, G. and Tuve, M.A. (1926) "A Test of the Existence of the Conducting Layer", Physical Review, 28(3), 1926, pp. 554-575.

Davies, K. (1965) Introduction to HF Radio Propagation published by US Dept. of Commerce, National Bureau of Standards, Washington D.C. 20402. Ark:/13960/t64484g1h pp. 149-150 & 276

Gillard, T. R. et al Characteristics of the Ionosphere and their Application to Radio Transmission Proc. IRE, 25, 823-840, 1937.

Grotz, Toby "The True Meaning of Wireless Transmission of power". Tesla : A Journal of Modern Science, 1997.

Gwyn Williams "Interpreting Digital Ionograms", RadCom, Radio Society of Great Britain, 85(05), May 2009, pp. 44-46.

Hargreaves, J. K. "The Upper Atmosphere and Solar-Terrestrial Relations". Cambridge University Press, 1992,

Jacobs, G., et al "The new Shortwave Propagation Handbook", CQ Communications, Inc., ISBN 0-943016-11-8, 1995, pages 1-2 to 1-5.

John S. Belrose "Fessenden and Marconi: Their Differing Technologies and Transatlantic Experiments During the First Decade of this Century".

International Conference on 100 Years of Radio -- 5-7 September 1995.

Judd, F.C. "Radio Wave Propagation (HF Bands)", Heinemann, London, ISBN 0-434-90926-2, 1987, pages 12–20, 27–37

Kelley, M. C., et al "The Earth's Ionosphere: Plasma Physics and Electrodynamics". Academic Press, 1989.

Lehtoranta, V.K. YLE - Finnish Broadcasting Corporation, Network Planning Services (ret.), personal communications Copyright 2002...2010 Ilkka Yrjölä First edition 10062002 Latest revision 14062002

Leo F. McNamara. (1994) ISBN 0-89464-804-7 "Radio Amateurs Guide to the Ionosphere".

Odishaw, H. (1961) The challenge of new horizons in science. Sci. Ed., 45: 16–20. doi:10.1002/sce.3730450108

Randy M. Russell (2003) www.windows2universe.org/bio/randy_russell.html

Rawer, K. Wave Propagation in the Ionosphere. Kluwer Acad.Publ., Dordrecht 1993. ISBN 0-7923-0775-5

Rishbeth, H. et al Introduction to Ionospheric Physics, Academic Press N. Y. 165 -185, 1969.

Yenne, Bill (1985). The Encyclopedia of US Spacecraft. Exeter Books (A Bison Book), New York. ISBN 0-671-07580-2. p.12 AEROS

Yuen, P. C. et al Diurnal Variation of the Ionospheric TEC, J. Geophysical Research, 71(3), 849 – 854, 1966.